

**APPENDIX A**  
**GEOPHYSICAL SURVEY REPORT**

**Geophysical Survey Report  
GSA Warehouse Area  
Parcels 151(7), 2(7), 3(7), 4(7), 67(7), 69(7), 238(7), 129(7),  
111(7), 91(7) and 128(7)**

**Fort McClellan, Alabama**

**October 2000**

The statements, opinions, and conclusions contained in this report are based solely upon the services performed by IT Corporation (IT) as described in this report and the Scope of Work as established for the report by the Client's budgetary and time constraints and the terms and conditions of the agreement with Client. In performing these services and preparing the report, IT relied upon work and information provided by others, including public agencies, whose information is not guaranteed by IT.

The findings of the report are limited to those specifically expressed in the report and no other representations or warranties are given by IT and no additional conclusions should be reached or representations relied on other than those expressly stated in the report and as limited by IT Terms and Conditions.

# Table of Contents

---

	<i>Page</i>
List of Figures.....	ii
List of Acronyms.....	iii
A.1.0 Introduction.....	A-1-1
A.2.0 Field Procedures.....	A-2-1
A.2.1 Survey Control.....	A-2-1
A.2.2 Geophysical Survey.....	A-2-1
A.2.2.1 Magnetic Survey.....	A-2-3
A.2.2.2 Time-Domain EM Survey.....	A-2-3
A.2.2.3 Frequency-Domain EM Survey.....	A-2-4
A.2.2.4 Anomaly Verification and GPR Survey.....	A-2-5
A.3.0 Data Processing.....	A-3-1
A.4.0 Interpretation of Geophysical Data.....	A-4-1
A.4.1 Data Interpretation Criteria.....	A-4-1
A.4.2 GSA Warehouse Area Data Interpretation.....	A-4-3
A.5.0 Conclusions and Recommendations.....	A-5-1
Attachment - Theoretical Background	

## List of Figures

---

<b>Number</b>	<b>Title</b>	<b>Follows Text</b>
A-1	Vicinity Map	
A-2	Site Map with Geophysical Interpretation	
A-3	Contour Map of G-858G Total Magnetic Field, Upper Sensor	
A-4	Contour Map of the Analytic Signal Calculated from G-858G Upper Sensor Data	
A-5	Contour Map of EM61 Bottom Coil (N-S Survey Lines)	
A-6	Contour Map of EM61 Bottom Coil (E-W Survey Lines)	
A-7	Contour Map of EM31 Conductivity (N-S Survey Lines)	
A-8	Contour Map of EM31 In-Phase Component (N-S Survey Lines)	
A-9	Contour Map of EM31 Conductivity (E-W Survey Lines)	
A-10	Contour Map of EM31 In-Phase Component (E-W Survey Lines)	
A-11	GPR Line 65E, 400-MHz Antenna	
A-12	GPR Line 75E, 400-MHz Antenna	
A-13	GPR Line 75N, 400 MHz Antenna	
A-14	GPR Line 180N, 400 MHz Antenna	

## List of Acronyms

---

CD	compact disk
E-W	east to west
EBS	Environmental Baseline Study
EM	electromagnetic induction
EM31	Geonics Limited EM31 Terrain Conductivity Meter
EM61	Geonics Limited EM61 High-Resolution Metal Detector
ESE	Environmental Science and Engineering, Inc.
FMP 1300	Former Motor Pool 1300 Site
FTMC	Fort McClellan
G-856	Geometrics, Inc. G-856 magnetometer
G-858G	Geometrics, Inc. G-858G magnetic gradiometer
GPR	ground penetrating radar
GPS	global positioning system
GSSI	Geophysical Survey Systems Inc.
IT	IT Corporation
MHz	megahertz
mS/m	millisiemens per meter
mV	millivolts
NAD	North American Datum
ppt	parts per thousand
N-S	north to south
ns	nanoseconds
nT	nanoteslas
RTK	real-time kinematic
SSFSP	Site-Specific Field Sampling Plan
TERC	Total Environmental Restoration Contract
USACE	U.S. Army Corps of Engineers
UST	underground storage tank

## ***A.1.0 Introduction***

---

IT Corporation (IT) conducted a surface geophysical survey at the GSA Warehouse Area, [Parcels 151(7), 2(7), 3(7), 4(7), 67(7), 69(7), 238(7), 129(7), 111(7), 91(7) and 128(7)] at Fort McClellan (FTMC) in Calhoun County, Alabama, from October 5 through October 21, 1998, March 9 through March 16, 1999, and May 8, 1999. This survey was conducted for the U.S. Army Corps of Engineers (USACE) – Mobile District, under Total Environmental Restoration Contract (TERC) No. DACA21-96-D-0018, Delivery Order CK005. The geophysical survey objective was to locate buried metal potentially representing a 10,000-gallon underground storage tank (UST). Based on the criteria established in the Site-Specific Field Sampling Plan (SSFSP) for UST identification, anomalies that are a typical size for a 10,000-gallon UST (8 ft by 28 ft or 10 ft by 18ft) and are located in logical areas (i.e., adjacent to typical FTMC gas station foundations) are identified and labeled as USTs. Anomalies that are either a typical size or in a logical location for a UST are labeled as potential USTs. The area surveyed was approximately 25,500 square feet (0.58 acres). The Vicinity Map (Figure A-1) shows the approximate location of the survey area.

To accomplish the objectives of the investigation, an initial site-screening survey was conducted using magnetic and electromagnetic (EM) methods. Ground penetrating radar (GPR) was later used in an effort to discriminate between magnetic and EM anomalies caused by the target USTs and those caused by other subsurface features, such as utility vaults, or pits containing significant metallic debris. All geophysical data were processed and color-enhanced to aid in interpreting subtle anomalies. Following geophysics fieldwork, a survey-grade global positioning system (GPS) was used to document the location of the site.

This site has relatively flat topography. The survey area is primarily grass and asphalt covered with a concrete sidewalk, as shown on the site map with geophysical interpretation (Figure A-2).

Field procedures used during the investigation are described in Chapter A.2.0. The data processing methods used during the investigation are presented in Chapter A.3.0. Data interpretation and techniques used to rank geophysical anomalies as to their potential to be caused by tanks is presented in Chapter A.4.0. Conclusions and recommendations derived from the geophysical surveys are presented in Chapter A.5.0. A description of the equipment and a theoretical discussion of the geophysical methods are presented in the Attachment.

## ***A.2.0 Field Procedures***

---

This chapter describes the field procedures and instruments used to conduct the investigation, including survey control, data acquisition, and field verification of geophysical anomalies.

### ***A.2.1 Survey Control***

The geophysical survey area was identified in the site specific work plan based on historical site information compiled by IT and the Environmental Baseline Study (EBS), (ESE, 1998). The geophysics crew established a base grid on 100-foot centers throughout the site. Using the base grid as a reference, the crew marked control points on 10-foot centers with surveyor's paint to provide the spatial control required for the investigation. Due to the uncertainty of true field positions inherent when establishing a survey area using 300-foot fiberglass tapes in the presence of wind and surface obstructions (e.g., trees, vehicles, and structures), the lateral precision for the survey areas and anomalies is estimated to be within +/- 1 foot. Following geophysics field work, a GPS survey was conducted at the site referencing the U.S. State Plane Coordinate System (Alabama East Zone, North American Datum [NAD]1983). The GPS survey was performed in the real-time kinematic (RTK) mode, which provided nominal sub-centimeter resolution in XY coordinates for the site.

A detailed site map was hand-drawn in the field. The map included any surface cultural features within the survey area, or near its perimeter, that could potentially affect the geophysical data (e.g., vehicles, overhead utilities, manhole covers). The map also shows reference features, such as buildings, fences, asphalt patches, and survey monuments that could later aid in reconstructing the site boundaries. All pertinent reference information documented on the hand-drawn site map was placed on the site interpretation map (Figure A-2). Also included on the site map are GPS coordinates to help relocate the survey area.

### ***A.2.2 Geophysical Survey***

***Field Instruments.*** The magnetic instruments used during the investigation consisted of a Geometrics Inc. G-858G magnetic gradiometer (G-858G) for collecting survey data and a Geometrics G-856 for collecting magnetic base station data. Time-domain EM induction equipment consisted of a Geonics EM61 High-Resolution Metal Detector coupled to an Omnidata DL720 digital data logger. Frequency-domain EM induction equipment consisted of a

Geonics EM31 Terrain Conductivity Meter (EM31) coupled to an Omnidata DL720 digital data logger. Ground penetrating radar equipment consisted of a Geophysical Survey Systems Inc. (GSSI) Model SIR-2P unit coupled to 200- and/or 400-megahertz (MHz) antennae and a DPU-5400 thermal gray-scale printer. Where required, a Metrotech 9860-BRL EM utility locator was used to verify that linear anomalies seen in the EM31/EM61 data were caused by subsurface pipelines or utilities. A Trimble 4000SSI Total Station GPS was used to conduct the civil survey work.

All geophysical data were collected using the following IT standard operating procedures:

- ITGP-001 Surface Magnetic Surveys
- ITGP-002 Surface Frequency-Domain Electromagnetic Surveys
- ITGP-003 Ground Penetrating Radar Surveys
- ITGP-004 Surface Time-Domain Electromagnetic Surveys
- ITGP-005 Global Positioning System Surveys
- ITGP-012 Geophysical Data Management.

The three geophysical techniques of magnetics, time-domain EM, and frequency-domain EM, were used initially to screen the survey area for large buried metal objects the size of a UST. These combined methods offer the technical approach most likely to succeed in locating and delineating large metal objects. Following magnetic and EM data processing and interpretation, GPR data was used to aid with interpreting the anomalies observed in the magnetic and EM maps. The GPR survey was focused only on those anomalies potentially caused by a UST.

***Field Instrument Base Station.*** A field instrument base station was established at GSA to provide quality control for the geophysical survey data collected at the site. The base station location was chosen to be free of surface and subsurface cultural features that could affect the geophysical data. Standard field procedures were to occupy the base station and collect readings with the survey instruments (magnetic, EM31, and EM61) before and after each data collection session. These before and after base station files were then reviewed to assess instrument operation. Base station file names and average data values within them were recorded on base station summary forms.

### **A.2.2.1 Magnetic Survey**

**Magnetic Base Station.** A magnetic base station was established at FTMC to record the background fluctuation (diurnal drift) of the Earth's magnetic field. The magnetic base station was located in a field of small pine trees on the south side of Sixth Avenue (near Parcel 151), a location which was determined to be free of surface and subsurface cultural features that could affect the data. A G856-AX magnetometer was used for the magnetic base station, however, instrument problems prevented collecting adequate background magnetic field data to "drift correct" the survey data. Regional magnetic field data from the time of data collection were reviewed, and it was determined that the survey was conducted during a time of quiescence.

**G858-G Data Collection.** Magnetic field measurements were made with the two sensors of the G858-G spaced 2.5 feet (0.76 meters) apart; the lower sensor was 2.0 feet above the ground surface and the upper sensor was 4.5 feet above the ground surface. At the start and end of each data collection session, approximately 60 readings were recorded with the G-858G at the field instrument base station to verify that the instrument was operating properly, and to provide a quantitative record of instrument variation during the survey period. A review of these base station files indicates that the instrument was operating properly and the instrument drift was within acceptable limits. Magnetic survey data were collected at 0.5-second intervals (approximately 2.0- to 2.5-foot intervals) along north to south (N-S) oriented survey lines spaced 10 feet apart, for a total of approximately 2,760 linear feet of survey coverage.

The magnetic data were stored in the internal memory of the G-858G, along with corresponding line and station numbers and the time of acquisition. Magnetic survey data were screened in the field to assess data quality prior to completing the investigation. All magnetic survey and base station data were downloaded to a personal computer, backed up on IOMEGA® compatible zip disks, and are retained in project files.

### **A.2.2.2 Time-Domain EM Survey**

**EM61 Data Collection.** Prior to conducting the EM61 survey, the instrument was calibrated to read zero at the field instrument base station. The EM61 was operated in the wheel mode with manual triggering and measurements of the potential difference in the top and bottom coils were collected. At the start and end of each data collection session approximately 20 readings were recorded at the field instrument base to verify that the instrument was operating properly, and to

provide a quantitative record of instrument variation, or drift, during the survey period. A review of these base station files indicates that the instrument was operating properly and instrument drift was within acceptable limits. Survey data were collected at 2.5-foot intervals along N-S and east to west (E-W) oriented survey lines spaced 5 feet apart, for a total of approximately 10,560 linear feet of survey coverage. The EM61 data were acquired along perpendicular survey lines to define anomalies potentially caused by subsurface utilities, thereby improving the geophysical interpretation of EM61 anomalies as they relate to possible USTs.

The EM61 data were stored in the digital data logger with corresponding line and station numbers. EM61 line profiles were reviewed in the field using the DAT61<sup>®</sup> program to verify data quality prior to completing the survey. All EM61 survey and base station data were downloaded to a personal computer, backed up on IOMEGA compatible zip disks, and are retained in project files.

### ***A.2.2.3 Frequency-Domain EM Survey***

***EM31 Data Collection.*** Prior to conducting the EM31 survey the instrument was calibrated and the in-phase component zeroed at the field instrument base station. The instrument was operated in the vertical dipole mode measuring the in-phase and out-of-phase components of the secondary EM field. At the start and end of each data collection session approximately 20 readings were recorded at the field instrument base station to verify that the instrument was operating properly, and to provide a quantitative record of instrument variation, or drift, during the survey period. A review of these base station files indicates that the instrument was operating properly and instrument drift was within acceptable limits. Survey data were collected at 5-foot intervals along N-S and E-W oriented survey lines spaced 10 feet apart, for a total of approximately 5,610 linear feet of survey coverage. The EM31 data were acquired along perpendicular survey lines to provide a clear definition of anomalies potentially caused by subsurface utilities, thereby improving the geophysical interpretation of EM31 anomalies as they relate to possible USTs.

The EM31 data were stored in the digital data logger along with corresponding line and station numbers. EM31 line profiles were reviewed in the field using the DAT31<sup>®</sup> program to verify data quality prior to completing the survey. All EM31 survey and base station data were downloaded to a personal computer, backed up on IOMEGA<sup>®</sup> compatible zip disks, and are retained in project files.

#### **A.2.2.4 Anomaly Verification and GPR Survey**

**Anomaly Verification.** Preliminary color-contour maps of the magnetic, EM61, and EM31 data were generated and field-checked to differentiate between anomalies caused by surface and subsurface sources. Geophysical anomalies verified as being caused by surface features were labeled as such on the field data maps. Geophysical anomalies suspected to be caused by underground utilities were verified with an EM utility locator. The locations of confirmed utilities were placed on the site map. Anomalies caused by buried metallic objects potentially representing a UST were carefully located in the field and marked on the site map for further characterization with GPR.

**GPR Data Collection.** Ground penetrating radar data were collected to discriminate between EM and magnetic anomalies potentially caused by USTs from those caused by significant buried metallic debris, metal reinforced utility vaults and junction boxes and localized concentrations of metal. GPR data is also useful to identify USTs near objects such as buildings, fences, and reinforced concrete pads which tend to mask the signature of the UST in the EM and magnetic data. The GPR survey included acquisition of 13,210 linear feet of data using the 200- and 400-MHz antennas. The digital GPR data were recorded continuously (32 scans per second) as the antenna was hand-towed across the survey lines. Control points were marked on the GPR records using a marker switch located on the antenna unit. The GPR data were field-reviewed in real time on a color monitor, stored in the internal memory of the instrument, and later downloaded to a personal computer. The GPR data were printed in the field as the survey progressed using a high-resolution thermal gray-scale printer. All GPR survey data were backed up on compact discs (CD), and are retained in project files.

## **A.3.0 Data Processing**

---

**Color Contour Maps.** Plots of magnetic, EM61, and EM31 data were generated using the OASIS Montaj® geophysical mapping system and UX-Detect® from Geosoft, Inc. These maps were color-enhanced to aid with interpreting subtle anomalies. Select contour maps from this site are presented as Figures A-3 through A-10.

A series of data processing steps were required to generate the contour maps. Magnetic gradiometer data was downloaded from the field instrument and converted to an ASCII file using Geometrics, Inc. MAGMAP® program. EM31 and EM61 data were downloaded from the data loggers and converted to ASCII files using DAT31 and DAT61 software from Geonics, Inc. The ASCII data files were then reviewed to assess line numbers, station ranges, and overall data quality. Field data file names and corresponding base station data files were recorded on the data file tracking form. Data screening results were then recorded on the base station summary form. Following data quality assessment, geometry corrections to field data files were made, if necessary, using a text editor and recorded on the geophysical data editing form.

Final, corrected magnetic and EM data files containing local geophysical station coordinates (X,Y) and the geophysical measurement (Z) were converted to OASIS Montaj® format and imported into the geophysical mapping software. The data were then gridded using bi-directional gridding with an Akima spline. The grid cell size for the magnetic, EM61, and EM31 data was chosen to be 2.5, 1.25, and 2.5 feet, respectively. Color-contouring was used to enhance data anomalies. The magnetic data were also processed using Geosoft Inc.'s UX-Detect® software to aid in determining the location of anomaly sources.

Due to the number and complexity of the magnetic anomalies, additional processing beyond the capabilities of OASIS Montaj® was conducted on the magnetic field data using the Geosoft UX-Detect® interpretation software. The UX-Detect® software performs inverse modeling by calculating 3D gradients of the magnetic data, determining the peak gradient locations, and then performing Euler deconvolution to solve for the apparent depth of the source material of the anomaly. With the calculated depths, and the known magnetic field above the sources, the software uses a look-up table to find the apparent weights of the sources. The results of the UX-Detect® processing are generated in a table that lists the X,Y position of the source object(s), as well as their apparent depths and weights. This table can then be sorted to exclude (or include)

sources with particular sizes and depths. Literature provided by Geosoft, Inc., states that the look-up table used to estimate weights of source materials was created for ordnance and projectiles, and, as such, can overestimate the weight of other steel objects. Therefore, each anomaly requires independent verification by the data processor as being reasonable.

The upper sensor magnetic data are considered more useful than the lower sensor data for locating metallic objects, such as steel drums, because the upper sensor is less influenced by small and near-surface objects. Hence, the upper sensor data were used in enhanced processing and analysis. The lower sensor total magnetic field data, when combined with the upper sensor data (i.e., vertical magnetic gradient), are most useful for determining the relative depth of burial of metallic source objects. The Analytic Signal calculated from the upper sensor magnetic data (Figure A-4) was gridded and shaded using the UX-Detect<sup>®</sup> bi-directional gridding module with Akima spline. The grid cell size was 2.5 feet

The names of files generated and processing parameters used were recorded on data processing forms. Final processed map names are shown in the data processing box found in the lower left corner of each contour map presented. All completed forms of magnetic and EM data collected during the investigation are retained in project files.

**GPR Profiles.** Select GPR data were processed using Gradix<sup>®</sup> data processing and interpretation system from Interpex Limited, and are presented as Figures A-11 through A-14. The GPR data were trace balanced and gained using an automatic gain control (AGC) function. A color amplitude function was then chosen to enhance features of interest. Following GPR processing, the data were imported to MICROSOFT Word<sup>®</sup> to produce color figures. GPR data file names are shown in the lower left of each profile. All GPR data are stored on CDs and retained in project files.

## ***A.4.0 Interpretation of Geophysical Data***

---

The methods by which the geophysical data were interpreted, and the results of that interpretation are described in this chapter.

Figure A-2 presents the site map with geophysical interpretation. The interpreted color-contour map of total magnetic field for the upper sensor is presented as Figure A-3. The UX-Detect analytical signal map is presented as Figure A-4. Interpreted color-contour maps of EM61 bottom coil data acquired along N-S and E-W survey lines are presented as Figures A-5 and A-6, respectively. Interpreted color-contour maps of EM31 conductivity and in-phase component data collected along N-S survey lines are presented as Figures A-7 and A-8, respectively. Interpreted color-contour maps of EM31 conductivity and in-phase component data collected along E-W survey lines are presented as Figures A-9 and A-10, respectively. Four GPR profiles are presented to show that due to site conditions GPR was unsuccessful in helping to determine anomaly sources (Figures A-11 through A-14). The locations of these GPR profiles are shown on Figure A-2. A theoretical background is presented as an Attachment to this appendix. This attachment discusses the factors influencing the observed geophysical response for the various methods used.

In addition to the geophysical interpretation and GPR line locations, the site map (Figure A-2) contains detailed information on reference features (e.g., asphalt and concrete pavement, buildings, and fences), so that the survey area and the geophysical anomaly locations can be relocated in the future. Anomalies shown on the site interpretation map correspond to those seen in the magnetic, EM, and GPR data. Surface reference features shown on the site interpretation map were translated from the hand-drawn site map made in the field. The site interpretation map also references the Alabama East State Plane, North American Datum 1983 Coordinate System.

### ***A.4.1 Data Interpretation Criteria***

***Color Contour Map Anomalies.*** Anomalies shown on the magnetic and EM contour maps range from high to low values and from negative to positive, depending on the type of data displayed. The observed anomalies in the contour map of total magnetic field for the upper sensor have values above and below the average magnetic field intensity of 50,800 nanoteslas (nT) for Anniston, Alabama. The typical magnetic data response to near-surface ferrous metallic

debris is an asymmetric south high/north low signature. The upper sensor magnetic data are more useful than the lower sensor data for locating large buried objects, such as USTs because the lower sensor is more sensitive to small near-surface objects; hence the upper sensor magnetic data are presented. The characteristic EM61 response over a buried metal object shows a positive-amplitude signal, with signal strength dependent upon the size of the object, distance from the transmitter/receiver coils, and the type of material. Upper and lower receiver coils readings can be processed to determine a differential value that can be used to determine the depth of source objects in the data. Although all EM61 data were evaluated during interpretation, only the bottom coil EM61 data is presented in the report because it is the most sensitive to buried metal objects. The characteristic EM31 anomaly over a near-surface metallic conductor consists of a narrow zone having strong negative amplitude centered over the target and a broader lobe of weaker, positive amplitude on either side of the target. As the depth of the target feature increases, the characteristic EM31 response changes to a positive amplitude centered over the target.

Anomalies present on the contour maps of magnetic, EM61, and EM31 data were first field-checked and correlated with known metallic surface objects and other cultural surface features so that anomalies caused by subsurface sources could be determined. Many of the high-amplitude anomalies seen in the contour maps of the magnetic, EM61, and EM31 data (Figures A-3 through A-10) are caused by cultural features including fences, buildings, underground utilities, and metallic debris. These anomalies, as well as anomalies identified to be caused by source objects the size of a UST, are labeled on each of the contour maps and are discussed in the following text. Several anomalies interpreted to be caused by discrete, buried metal objects smaller than a UST are not discussed in the text.

Figure A-4 was created using Geosoft's UX-Detect®. UX-Detect® was used to aid in determining the location of the anomaly sources. It is difficult to identify the target in the total magnetic field data and to locate the center of the source due to the complexity of the geometry and the magnetic characteristics of the source. The source can be located because the permanent magnetism of a man-made source differs from the Earth's magnetic field. The magnetic gradient data show the high frequency component and often resolves a magnetic anomaly into smaller anomalies defining the source boundaries.

***UST Anomaly Identification.*** Each anomaly potentially caused by a UST is designated by a numeric symbol on the geophysical interpretation map, color-contour maps, and GPR profiles.

The number shown in parenthesis indicates the anomaly type and potential for the source object to be a UST.

According to the SSFSP criteria anomalies that are found of typical size and in logical areas for USTs (i.e., adjacent to typical FTMC gas station foundations) will be identified and labeled as USTs. Anomalies that are of typical sizes but not in logical locations will be labeled as potential USTs.

Anomalies were identified using test pits or direct push sampling methods to determine the presence or absence of a UST(s).

#### ***A.4.2 GSA Warehouse Area Data Interpretation***

Twelve geophysical anomalies not explained by known surface or subsurface cultural features are labeled on the data maps and are discussed in the following text.

***Anomaly A-1.*** Anomaly A-1 is located at (60E, 185N) and occurs in all three site-screening methods of investigation. The anomaly shows a high-amplitude response in both the magnetic and EM31 data (Figures A-3, A-4, A-7, A-8, A-9, and A-10) and has a moderate-amplitude response in the EM61 data (Figures A-5 and A-6). Anomaly A-1 is interpreted from the analytic signal data (Figure A-4) to have a source approximately 10 feet deep. The source of the anomaly is not visible in the GPR data (Figures A-11, A-12 and A-14). Anomaly A-1 could be caused by a UST, but it could also be caused by a transfer pit, valve box, or a utility corridor. Although it is likely that the anomaly is a UST, according to the criteria established in the SSFSP for UST identification, Anomaly A-1 is a potential UST since it does represent a typical size for a 10,000-gallon UST, but is not located in a logical area for a UST.

***Anomaly A-2.*** Anomaly A-2 is located at (80E, 210N) and occurs in all three site-screening methods of investigation. The anomaly has a moderate-amplitude response in all the data sets. In the magnetic data (Figure A-3) and the EM61 data (Figures A-5 and A-6) the anomaly signature is not fully delineated. The interpretation map (Figure A-2) notes A-2 and approximates its northern boundary. Anomaly A-2 is thought to have a source approximately 6 feet deep (Figure A-4). The response in the EM31 data is difficult to determine due to interference from Anomaly A-1, Anomaly A-3, and a nearby pipe. Although Anomaly A-2 is possibly caused by a small UST, according to the criteria established in the SSFSP for UST

identification, Anomaly A-2 is not a UST since it does not represent a typical size for a 10,000-gallon UST, and is not located in a logical area for a UST.

**Anomaly A-3.** Anomaly A-3 is located at (78E, 185N) and occurs in all three site-screening methods of investigation. The anomaly has a high-amplitude response in all the data sets. It appears as a strong magnetic low (Figure A-3 and A-4) and a linear N-S feature in the EM61 data. Anomaly A-3 is interpreted to be 7-10 feet deep (Figure A-4). Anomaly A-3 and A-1 are seen as one large feature in the EM31 data (Figures A-7 through A-10). Although Anomaly A-3 could represent a UST, it could also be caused by a transfer pit, valve box, or a utility corridor. Two direct push samples were taken at this anomaly location and there was no evidence of a tank. Rebar material was found.

**Anomaly A-4.** Anomaly A-4 is located at (60E, 150N) and occurs in all three data sets. The anomaly has a high-amplitude magnetic dipole response (Figure A-3 and Figure A-4), a moderate-amplitude EM61 response (A-5 and A-6), and a high-amplitude response in the EM31 data (Figures A-7 through A-10). Anomaly A-4 is interpreted to have a source approximately 8 feet deep (Figure A-4). Although Anomaly A-4 could represent a UST, it could also be caused by a transfer pit, valve box, or a utility corridor. According to the criteria established in the SSFSP for UST identification, Anomaly A-4 is not a UST since it does not represent a typical size for a 10,000-gallon UST and is not located in a logical area for a UST.

**Anomaly A-5.** Anomaly A-5 is located at (83E, 156N) and appears as a moderate-amplitude anomaly in the magnetic and EM61 data sets (Figures A-3, A-4, A-9, and A-10, respectively). In Figure A-4 it is interpreted to have an approximate depth of 8 feet. Anomaly A-5 is seen in the EM31 data as a subtle low (Figures A-9 and A-10). Although Anomaly A-5 is possibly caused by a small UST, according to the criteria established in the SSFSP for UST identification, Anomaly A-5 is not a UST since it does not represent a typical size for a 10,000-gallon UST and is not located in a logical area for a UST.

**Anomaly A-6.** Anomaly A-6 is located at (85E, 130N) and appears in only the E-W EM31 data. The anomaly occurs as a high-amplitude in-phase anomaly (Figure A-10). A test pit was dug at this anomaly and no evidence of a tank was found.

**Anomaly A-7.** Anomaly A-7 is located at (60E, 115N) and occurs in all three site screening methods. The anomaly has a moderate to high-amplitude response in the data. It has an

interpreted depth of approximately 10 feet (Figure A-4). Although Anomaly A-7 could represent a UST, it could also be caused by a transfer pit, valve box, or a utility corridor. According to the criteria established in the SSFSP for UST identification, Anomaly A-7 is a potential UST since it does represent a typical size for a 10,000-gallon UST, but is not located in a logical area for a UST.

**Anomaly A-8.** Anomaly A-8 is located at (25E, 75N) and occurs in both the magnetic and EM31 data. The anomaly has a high-magnitude response in the magnetic data (Figure A-3). Anomaly A-8 appears to have a high-amplitude response in the EM31 conductivity data (Figures A-7 and A-9) and the EM31 in-phase data (Figures A-8 and A-10), but it is possible that the response is being affected by nearby pipes and reinforced concrete. The interpreted depth to the source object is approximately 7 feet (Figure A-9). The source of the anomaly is not visible in the GPR data (Figures A-11 and A-14). Anomaly A-8 could represent a UST, it could also be caused by a transfer pit, valve box, or a utility corridor. Although Anomaly A-8 is possibly caused by a UST, according to the criteria established in the SSFSP for UST identification, Anomaly A-8 is a potential UST since it does represent a typical size for a 10,000-gallon UST, but is not located in a logical area for a UST.

**Anomaly A-9.** Anomaly A-9 is located at (33E, 65N) and occurs in all three site screening methods. The anomaly has a moderate to high-amplitude response adjacent to typical pipeline responses. Although Anomaly A-9 could represent a UST, it could also be caused by a transfer pit or a valve box along the interpreted pipeline. According to the criteria established in the SSFSP for UST identification, Anomaly A-9 is not a UST since it does not represent a typical size for a 10,000-gallon UST and is not located in a logical area for a UST.

**Anomaly A-10.** Anomaly A-10 is located at (60E, 78N) and occurs in all data sets as a high amplitude anomaly. The magnetic response is dipolar in nature (Figure A-3) and the EM responses are large areas of high values (Figures A-5 through A-10). Anomaly A-10's depth estimate vary from 2-10 feet (Figure A-4). Four direct push samples were taken at this anomaly location and there was no physical evidence of a tank. Rebar material was found. Because the sample locations were placed primarily in the center of the anomaly, the possibility still exists that a tank exists within the anomalous area.

**Anomaly A-11.** Anomaly A-11 is centered at the approximate coordinates of (108E, 65N) and occurs in all three data sets as a moderate to high-amplitude anomaly. Anomaly A-11 has

interpreted depth to source ranging from 3 to 10 feet (Figure A-4). Although Anomaly A-11 could represent a UST, it could also be caused by a transfer pit or valve box associated with nearby pipelines. According to the criteria established in the SSFSP for UST identification, Anomaly A-11 is not a UST since it does not represent a typical size for a 10,000-gallon UST and is not located in a logical area for a UST.

**Anomaly A-12.** Anomaly A-12 is located at (140E, 80N) and occurs in all three data sets as a moderate to high amplitude anomaly. The depth to source has been interpreted to be approximately 6 feet (Figure A-4). Although Anomaly A-12 could represent a UST, it could also be caused by a transfer pit or valve box. According to the criteria established in the SSFSP for UST identification, Anomaly A-12 is not a UST since it does not represent a typical size for a 10,000-gallon UST and is not located in a logical area for a UST.

## ***A.5.0 Conclusions and Recommendations***

---

A surface geophysical survey using magnetic, EM and GPR methods was conducted from October 5 through October 21, 1998, March 9 through March 16, 1999, and May 8, 1999 at the GSA Warehouse Area. The objective of the survey was to locate buried metal representing a 10,000-gallon UST.

Twelve anomalies were identified in the geophysical data. Six of these anomalies are interpreted to represent potential USTs according to the criteria established in the SSFSP and three were examined using test pits or direct push sampling. Investigative methods did not indicate the presence of USTs. Rebar was found at two of the anomaly locations.

A hand drawn field map and GPS survey of site features provided a permanent record of the survey boundaries and anomaly locations. Positions on the site map generated (Figure A-2) are conservatively estimated to be accurate to within +/- 1 foot.

Pipeline locations are indicated on the site interpretation map where evident in the geophysical data. However, the map should not be considered clearance for exploratory trenching or other invasive investigations. Should such clearance be necessary, IT recommends proper geophysical clearance using available utility maps, EM utility locator, and GPR.

Beyond the recommendation above, and based on the objectives and results of the geophysical survey presented in this report, no further geophysical effort is recommended at the GSA Warehouse Area site.

**ATTACHMENT  
THEORETICAL BACKGROUND**

**Table of Contents**

---

	<b>Page</b>
List of Acronyms .....	ii
1.0 Magnetic Method.....	1
2.0 Frequency-domain Electromagnetic Induction Method.....	3
3.0 Time-domain Electromagnetic Induction Method .....	5
4.0 Ground-Penetrating Radar Method .....	6
5.0 References .....	8

## **List of Acronyms**

---

EM	electromagnetic induction
EM31	Geonics Limited EM31 Terrain Conductivity Meter
EM61	Geonics Limited EM61 High-Resolution Metal Detector
G-856	Geometrics Inc. G-856 Magnetometer
G-858G	Geometrics Inc. G-858G Magnetic Gradiometer
GPR	Ground Penetrating Radar
GSSI	Geophysical Survey Systems Inc.
9860-BRL	Metrotech Inc. 9860-BRL EM utility locator
mV	millivolts
mS/m	millisiemens/meter
MHz	megahertz
nT	nanoteslas
nT/m	nanoteslas/meter
ppt	parts per thousand
RF	radiofrequency
UXO	unexploded ordnance

## **1.0 Magnetic Method**

---

The magnetic instruments used during the Fort McClellan surface geophysical surveys were a Geometrics, Inc., G-858G "walking mode" magnetic gradiometer (G-858G) for acquiring survey data and a Geometrics, Inc., G-856 for collecting magnetic base station data.

The G-858G, which is an optically-pumped cesium vapor instrument, measures the intensity of the Earth's magnetic field in nanoteslas (nT) and the vertical gradient of the magnetic field in nanoTeslas per meter (nT/m). The vertical gradient is measured by simultaneously recording the magnetic field with two sensors at different heights. To determine the vertical magnetic gradient, the upper sensor reading is subtracted from the lower sensor reading, and the result is then divided by the distance between the sensors. The distance between sensors for this investigation was 2.5 feet (0.76 meters). The vertical magnetic gradient measurement allows for better definition of shallower anomalies.

During operation of the G-858G magnetic gradiometer, a direct current is used to generate a polarized monochromatic light. Absorption of the light occurs within the naturally precessing cesium atoms found in the instrument's two vapor cells or sensors. When absorption is complete, the precessing atoms become a transfer mechanism between light and a transverse radiofrequency (RF) field at a specific frequency of light known as the Larmor frequency. The light intensity is used to monitor the precession and adjusts the RF allowing for the determination of the magnetic field intensity (Sheriff, 1991).

The Earth's magnetic field is believed to originate in currents in the Earth's liquid outer core. The magnetic field varies in intensity from approximately 25,000 nT near the equator, where it is parallel to the Earth's surface, to approximately 70,000 nT near the poles, where it is perpendicular to the Earth's surface. In Alabama, the intensity of the Earth's magnetic field varies from 50,000 nT to 51,000 nT and has an associated inclination of approximately 54 degrees.

Anomalies in the Earth's magnetic field are caused by induced or remnant magnetism. Remnant magnetism is caused by naturally occurring magnetic materials. Induced magnetic anomalies result from the induction of a secondary magnetic field in a ferromagnetic material (e.g., pipelines, drums, tanks, or well casings) by the Earth's magnetic field. The shape and amplitude

of an induced magnetic anomaly over a ferromagnetic object depend on the geometry, size, depth, and magnetic susceptibility of the object and on the magnitude and inclination of the Earth's magnetic field in the study area (Dobrin, 1976; Telford, et al., 1976). Induced magnetic anomalies over buried objects such as drums, pipes, tanks, and buried metallic debris generally exhibit an asymmetrical, south high/north low signature (maximum amplitude on the south side and minimum on the north). Magnetic anomalies caused by buried metallic objects generally have dimensions much greater than the dimensions of the objects themselves. As an extreme example, a magnetometer may begin to sense a buried oil well casing at a distance of greater than 50 feet.

The magnetic method is not effective in areas with ferromagnetic material at the surface because the signal from the surface material obscures the signal from any buried objects. Also, the presence of an alternating current electrical power source can render the signal immeasurable because of the high precision required in the measurement of the frequency at which the protons precess (Breiner, 1973). The precession signal may also be sharply degraded in the presence of large magnetic gradients (exceeding approximately 600 nT/m).

The magnetic field measured at any point on the Earth's surface undergoes low-frequency diurnal variation, called magnetic drift, associated with the Earth's rotation. The source of magnetic drift is mainly within the ionosphere, and its magnitude is sometimes large enough to introduce artificial trends in survey data. The G-856 base station magnetometer was used to record this drift for removal from the G-858G survey data during processing.

Applications of the magnetic method include delineating old waste sites and mapping unexploded ordnance (UXO), drums, tanks, pipes, abandoned wells, and buried metallic debris. The method also is useful in searching for magnetic ore bodies, delineating basement rock, and mapping subsurface geology characterized by volcanic or mafic rocks.

## **2.0 Frequency-Domain EM Method**

---

Frequency-domain electromagnetic induction equipment used during this investigation consisted of a Geonics EM31 terrain conductivity meter (EM31) coupled to an Omnidata DL720 digital data logger. The EM31 consists of a 12-foot-long plastic boom with a transmitter coil mounted at one end and a receiver coil at the other. An alternating current is applied to the transmitter coil, causing the coil to radiate a primary EM field. As described by Faraday's law of induction, this time-varying magnetic field generates eddy currents in conductive subsurface materials. These eddy currents have an associated secondary magnetic field with a strength and phase shift (relative to the primary field) that are dependent on the conductivity of the medium. The combined effect of the primary and secondary fields is measured by the receiver coil in-phase (in-phase) and 90 degrees out-of-phase (quadrature) with the primary field. Most geologic materials are poor conductors. Current flow through geologic materials takes place primarily in the pore fluids (Keller and Frischknecht, 1966); as such, conductivity is predominantly a function of soil type, porosity, permeability, pore fluid ion content, and degree of saturation. The EM31 is calibrated so that the out-of-phase component is converted to electrical conductivity in units of millisiemens per meter (mS/m) (McNeill, 1980), and the in-phase component is converted to parts per thousand (ppt) of the secondary field to the primary EM field. The in-phase component is a relative value that is generally set to zero over background materials at each site.

The depth of penetration for EM induction instruments depends on the transmitter/receiver separation and coil orientation (McNeill, 1980). The EM31 has an effective exploration depth of approximately 18 feet when operating in the vertical dipole mode (horizontal coils). In this mode, the maximum instrument response results from materials at a depth of approximately two-fifths the coil spacing (or, approximately 2 feet below ground surface with the instrument at the normal operating height of approximately 3 feet), providing that no large metallic features such as tanks, drums, pipes, and reinforced concrete are present. Single buried drums typically can be located to depths of approximately 5 feet, whereas clusters of drums can be located to significantly greater depths if background noise is limited or negligible. In the horizontal dipole mode (vertical coils), the EM31 has an effective exploration depth of approximately 9 feet and is most sensitive to materials immediately beneath the ground surface.

The EM31 generally must pass over or very near a buried metallic object to detect it. Both the out-of-phase and in-phase components exhibit a characteristic anomaly over near-surface

metallic conductors. This anomaly consists of a narrow zone having strong negative amplitude centered over the target and a broader lobe of weaker, positive amplitude on either side of the target. For long, linear conductors such as pipelines, the characteristic anomaly is as described when the axis of the coil (instrument boom) is at an angle to the conductor. However, when the instrument boom is oriented parallel to the conductor, a positive amplitude anomaly is obtained.

The application of frequency-domain EM techniques includes mapping conductive groundwater contaminant plumes in very shallow aquifers, delineating oil brine pits, landfill boundaries and pits and trenches containing buried metallic and nonmetallic debris, and locating buried pipes, cables, drums, and tanks.

### **3.0 Time-Domain EM Method**

---

Time-domain electromagnetic induction equipment used during this investigation consisted of a Geonics EM61 high-resolution metal detector (EM61) coupled to an Omnidata DL720 digital data logger. The EM61 consists of one transmitter and two receiver coils each 1-meter square. The transmitter and one receiver coil are co-incident within the instrument, the second receiver coil is separated by 0.5 meters (m). Comparison of the readings in the two receiver coils allows for discrimination between shallow and deeply buried metal objects. In operation, a pulse of current in the transmitter coil generates a primary magnetic field that induces eddy currents in nearby metallic conductors, as described by Faraday's law of induction. These eddy currents produce secondary magnetic fields that are measured by the time-dependant, decaying voltage they produce in the receiver coils. The internal electronics of the EM61 are designed such that readings are taken in a very narrow time window following transmitter turn-off. The measurement of secondary fields in the absence of a primary field allows for the high sensitivity measurements obtained with the system. Since the current ring diffuses down and outward, readings taken immediately after current shut-off are most affected by near-surface conditions and the later readings by the electrical properties of the deeper subsurface.

The EM61 is generally adjusted in the field to have a zero millivolts (mV) response over background conditions.

The EM61 depth of penetration depends primarily on the size of the target, and to a lesser degree on the type of metal (Geonics, 1997). The EM61 has an effective exploration depth in excess of 10 feet for locating large conductive features, such as tanks.

The EM61 generally must pass over, or very, near a buried metallic object to detect it. The EM61 characteristic anomaly consists of readings elevated 10 to 20 mV above background for small conductors and up to several thousand mV for large conductors, such as tanks. For mapping long, linear conductors, the EM61 data is most useful when measurements are taken perpendicular to the orientation of the conductor.

The application of near-surface time-domain EM techniques with instruments such as the EM61, includes detecting and mapping metallic objects (buried pipes, cables, drums, and tanks), and mapping the boundaries of landfill, pits or trenches containing buried metallic debris.

## ***4.0 Ground Penetrating Radar Method***

---

Ground penetrating radar (GPR) equipment used during this investigation consisted of a Geophysical Survey Systems, Inc. (GSSI) Model SIR-2P equipped with 200- and 400-megahertz (MHz) monostatic antennas, and a DPU-5400 high-resolution thermal gray-scale printer.

When conducting a GPR survey, an antenna containing both a transmitter and a receiver is pulled along the ground surface. The transmitter radiates short pulses of high-frequency (center frequencies in the range of 200 to 400 MHz) EM energy into the ground. The EM wave propagates into the subsurface at a velocity determined by the electromagnetic properties (primarily dielectric constant) of the medium through which the wave travels. When the wave encounters the interface of two materials having different electromagnetic properties, such as between soil and an underground storage tank (UST), a portion of the energy is reflected back to the surface where the receiver measures its amplitude and time of arrival. The magnitude of the reflection is an indication of the degree of contrast in the electrical properties of the interface producing the reflection—the greater the contrast, the greater the amplitude. The time of the reflection arrival indicates the relative depth of the source of the reflection. The reflection is often seen as a characteristic triplet that is the result of the receiving antenna response and of multiples generated along the propagation path. The received signal is transmitted to a control unit, displayed on a color monitor, and saved on the control unit's digital hard drive.

As predicted by Maxwell's equations for a propagating EM wave, two kinds of charge flow are generated by the associated alternating electric and magnetic fields (Ulriksen, 1982). The charge flows are conduction and displacement currents. The conduction current term is predominant at lower frequencies, and conduction currents are used in the EM induction method. At the higher frequencies used in the GPR method, the displacement current term becomes predominant because the high frequencies will set bound charges in motion, causing polarization.

The physical properties that describe the movement of charges by conduction and displacement currents are the conductivity and the dielectric constant of the medium, respectively. Conductivity is a measure of the ease with which charges and charged particles move freely through the medium when subjected to an external electric field. The dielectric constant, or its value normalized by the dielectric constant of free space called the relative dielectric constant, is a measure of

how easily a medium polarizes to accommodate the EM fields of a propagating wave (Keller and Frischknecht, 1966).

Although conductivity has a smaller effect on the transmission of EM waves emitted from a GPR unit, it has an important effect on the attenuation of the waves (Ulriksen, 1982). Highly conductive media will attenuate the EM signal rapidly and restrict depth penetration to the first several feet. Highly resistive (poorly conductive) media allow deeper penetration. The frequency of the transmitted waves also affects the depth of penetration. Lower frequencies penetrate deeper but have lower resolution, whereas higher frequencies can resolve smaller objects and soil layers at the expense of depth penetration. At many sites in the southeastern U.S., heavy clay soils are relatively conductive and depth of penetration is often limited to 5 feet or less. At some sandy sites, typical of coastal regions, GPR depth of penetration has exceeded 8 feet.

In unconsolidated materials, conduction occurs predominantly through pore fluids (Keller and Frischknecht, 1966). Therefore, changes in pore fluid content, porosity, permeability, and degree of saturation will affect reflected and refracted EM signals. Backfilled trenches, in which there may be different compaction densities relative to the surrounding area, can be identified by low to moderate amplitude reflections. When the target of a GPR survey is a metallic conductor such as metal pipes and cables, drums, tanks, or ammunition shells, the reflections have high amplitude because of the nearly complete reflection of the EM wave from the metallic conductor. Thus, the property of total reflection makes metallic targets well suited for detection within the range of the GPR unit. No reflections will occur from below the metallic conductor, although multiples are common. The edges of metallic reflectors will generally exhibit diffraction patterns as a result of the transmitting and the receiving antennae being unfocused and emitting and receiving from a 45-degree cone. The cone causes the radar to receive reflections from objects that are ahead of it, at times later than an object at the same depth directly below the antennae. As the radar approaches an object, the reflection becomes earlier in time, with the earliest reflection taking place when the radar is directly above the object. A complimentary pattern occurs as the antenna moves away from the object, resulting in the characteristic hyperbolic shaped anomaly on GPR profiles characteristic of small, subsurface metallic objects.

Applications of GPR include delineation of pits and trenches containing metallic and nonmetallic debris; location of buried pipes, drums, and USTs; and mapping of landfill boundaries and near-surface geology.

## 5.0 References

---

Breiner, S., 1973, *Applications Manual for Portable Magnetometers*, Geometrics, Sunnyvale, California.

Dobrin, M. B., 1976, *Introduction to Geophysical Prospecting*, MacGraw-Hill, New York, New York.

Keller, G. V. and F. C. Frischknecht, 1966, *Electrical Methods in Geophysical Prospecting*, International Series in Electromagnetic Waves, Volume 10, Pergamon Press, Oxford, England.

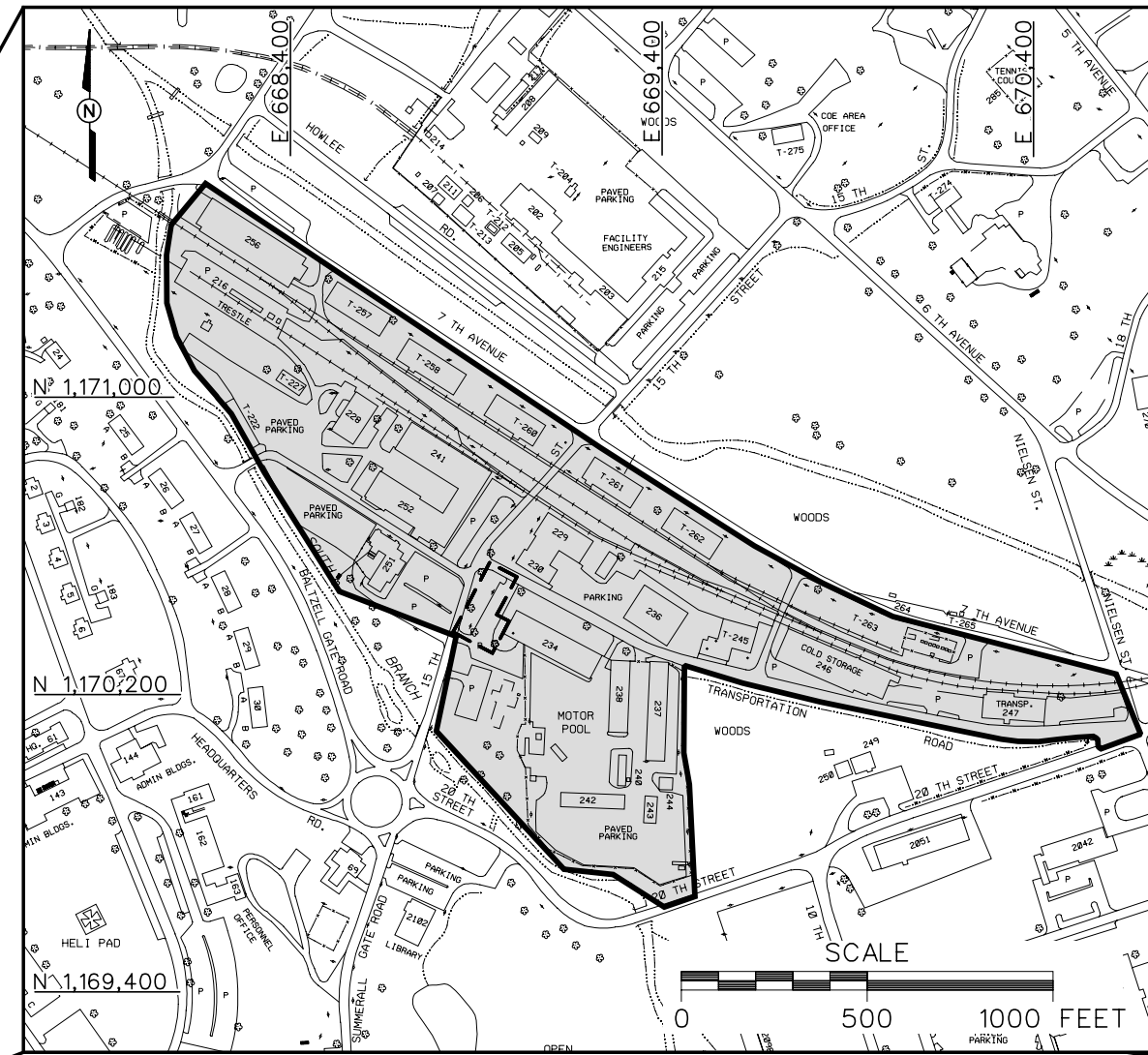
McNeill, J. D., 1980, *Electromagnetic Terrain Conductivity Measurement at Low Induction Numbers*, Geonics Limited, Technical Note TN-6, Ontario, Canada, October.

Sheriff, R. E., 1991, *Encyclopedic Dictionary of Exploration Geophysics*, Society of Exploration Geophysicists, Tulsa, Oklahoma.

Telford, W. M., L. P. Geldart, R. E. Sheriff, and D. A. Keys, 1976, *Applied Geophysics*, Cambridge University Press, Cambridge, England.

Ulriksen, C. P. F., 1982, *Application of Impulse Radar to Civil Engineering*, Department of Engineering Geology, Lund University of Technology, Sweden.

DWG. NO.: ... \774645es.250  
 PROJ. NO.: 774645  
 INITIATOR: M. MAKI  
 PROJ. MGR.: J. YACOUB  
 DRAFT. CHCK. BY:  
 ENGR. CHCK. BY: M. MAKI  
 DATE LAST REV.:  
 DRAWN BY:  
 STARTING DATE: 03/17/99  
 DRAWN BY: D. BILLINGSLEY  
 10/26/00  
 02:14:44  
 DBILLING  
 c:\cadd\design\774645es.250



- LEGEND**
- UNIMPROVED ROADS AND PARKING
  - PAVED ROADS AND PARKING
  - BUILDING
  - PARCEL 151(7) BOUNDARY
  - GEOPHYSICAL SURVEY AREA
  - SURFACE DRAINAGE / CREEK
  - FENCE
  - RAILROAD
  - UTILITY POLE

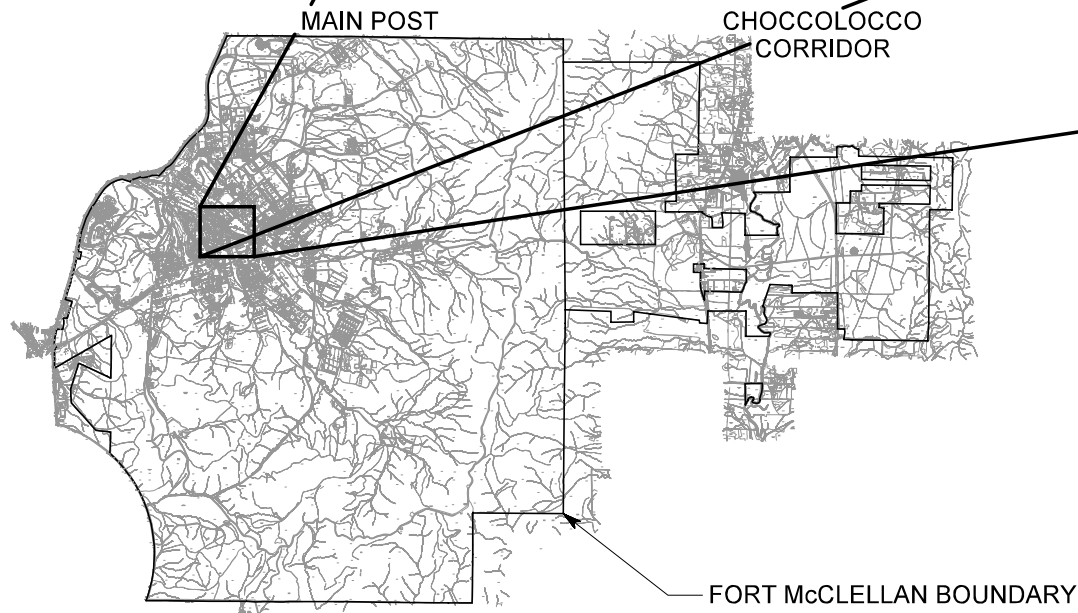
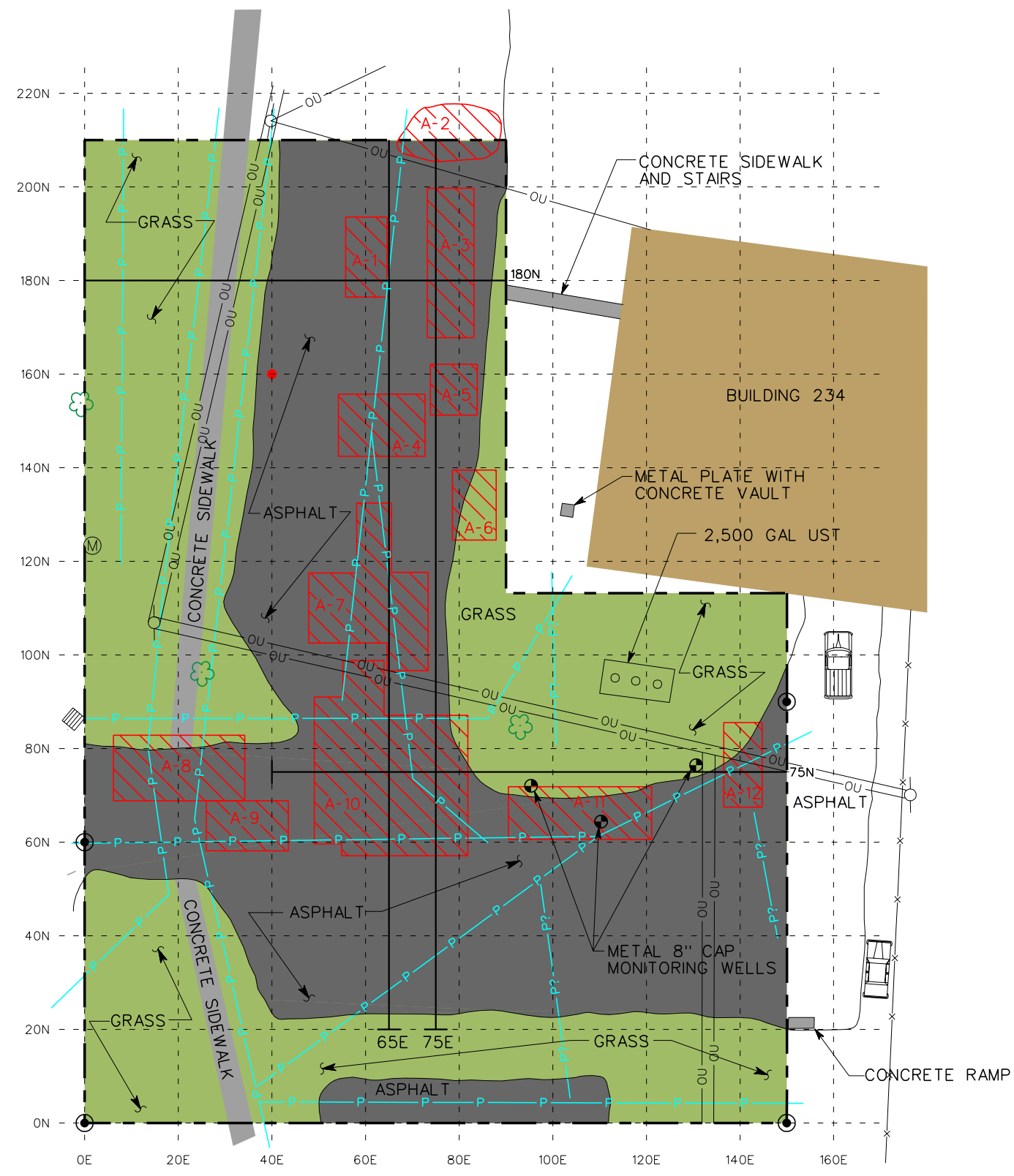
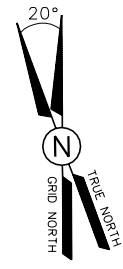


**FIGURE A-1**  
**VICINITY MAP**  
**GSA WAREHOUSE AREA**  
**PARCELS 151(7), 2(7), 3(7), 4(7),**  
**67(7), 69(7), 91(7), 111(7), 128(7),**  
**129(7), AND 238(7)**

U. S. ARMY CORPS OF ENGINEERS  
 MOBILE DISTRICT  
 FORT McCLELLAN  
 CALHOUN COUNTY, ALABAMA  
 Contract No. DACA21-96-D-0018



DWG. NO.: \774645es.459  
 PROJ. NO.: 774645  
 INITIATOR: S. TAKATA  
 PROJ. MGR.: J. YACOUB  
 DRAFT. CHECK. BY:  
 ENGR. CHECK. BY: J. HACKWORTH  
 DATE LAST REV.:  
 DRAWN BY:  
 STARTING DATE: 01/26/00  
 DRAWN BY: D. BILLINGSLEY  
 10/30/00  
 01:04:18  
 c:\cadd\design\774645es.459



**LEGEND**

- GEOPHYSICAL SURVEY BOUNDARY
- ⊙ CIVIL SURVEY STAKE LOCATION
- 75N GPR PROFILES PRESENTED
- GEOPHYSICAL ANOMALY DISCUSSED IN TEXT
- Ⓜ MANHOLE
- METAL GRATE
- UTILITY POLE
- PIPE/BURIED UTILITY
- OVERHEAD UTILITY LINES
- FENCE
- TREES / TREELINE
- METAL 8" CAP MONITORING WELL
- BURIED METAL

**NOTE**

1. LOCATIONS OF FEATURES OUTSIDE SURVEY AREA ARE APPROXIMATE.

NAD 83 SPHEROID, ALABAMA EAST STATE PLANE DATUM		
LOCAL GRID COORDINATES	STATE PLANE COORDINATES	
0N,0E	1170280.547N	668841.639E
0N,150E	1170228.771N	668982.052E
60N,0E	1170340.267N	668864.065E
90N,150E	1170315.196N	669014.736E

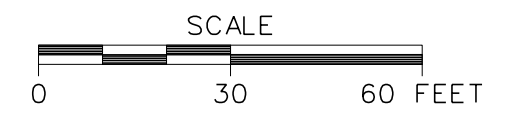
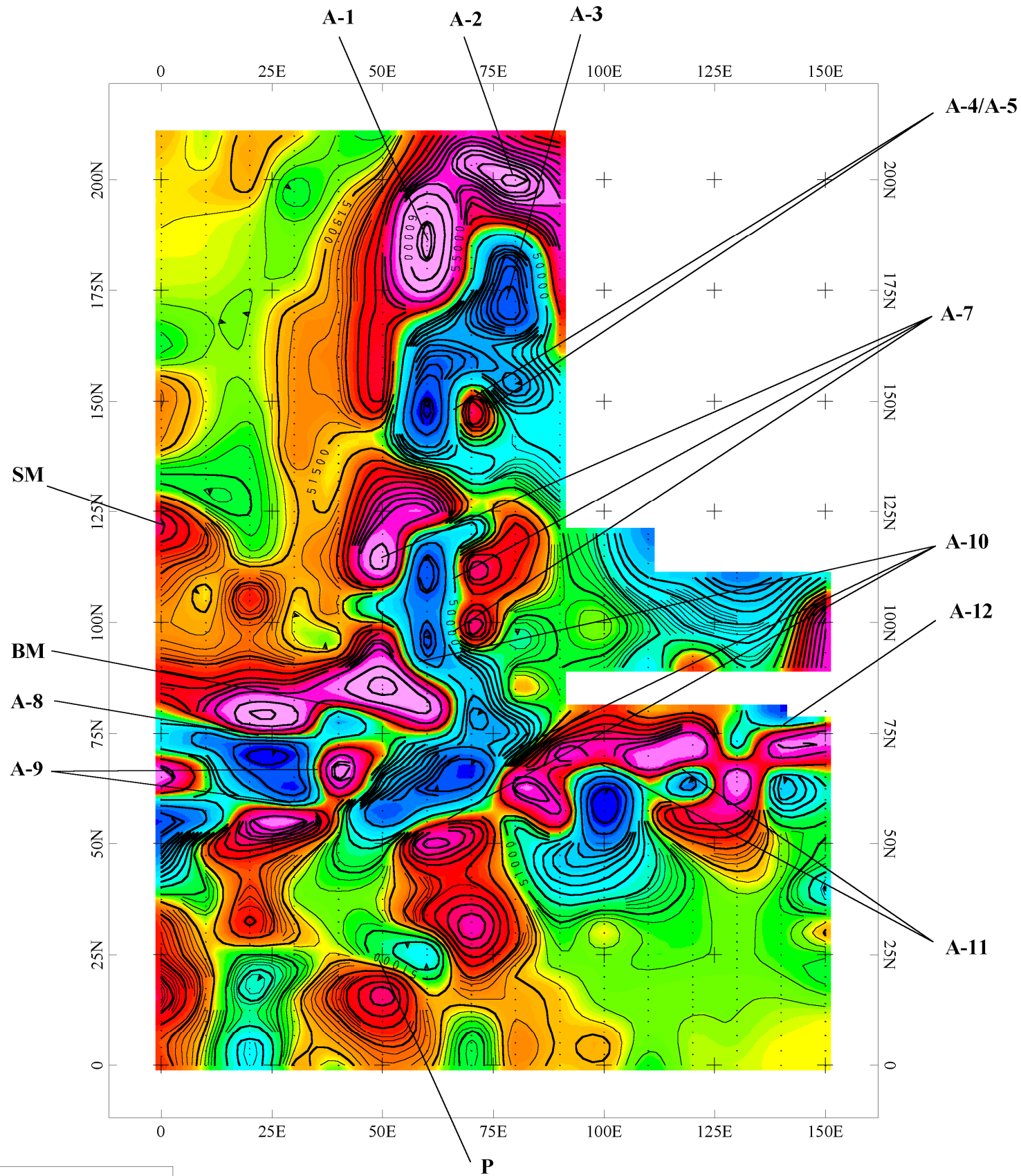
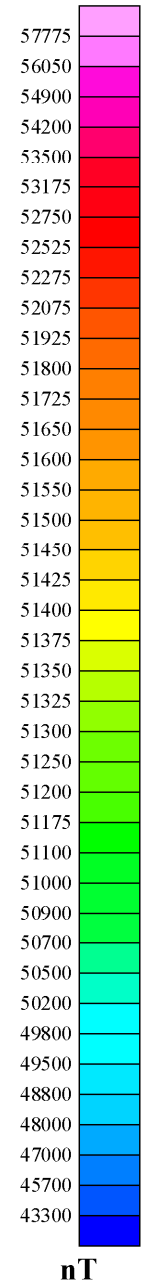


**FIGURE A-2**  
 GSA WAREHOUSE AREA  
 SITE MAP WITH GEOPHYSICAL  
 INTERPRETATION  
 PARCELS 151(7), 2(7), 3(7), 4(7),  
 67(7), 69(7), 91(7), 111(7), 128(7),  
 129(7) AND 238(7)

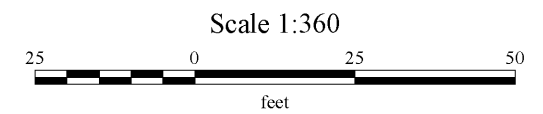
U. S. ARMY CORPS OF ENGINEERS  
 MOBILE DISTRICT  
 FORT McCLELLAN  
 CALHOUN COUNTY, ALABAMA  
 Contract No. DACA21-96-D-0018





**LEGEND:**

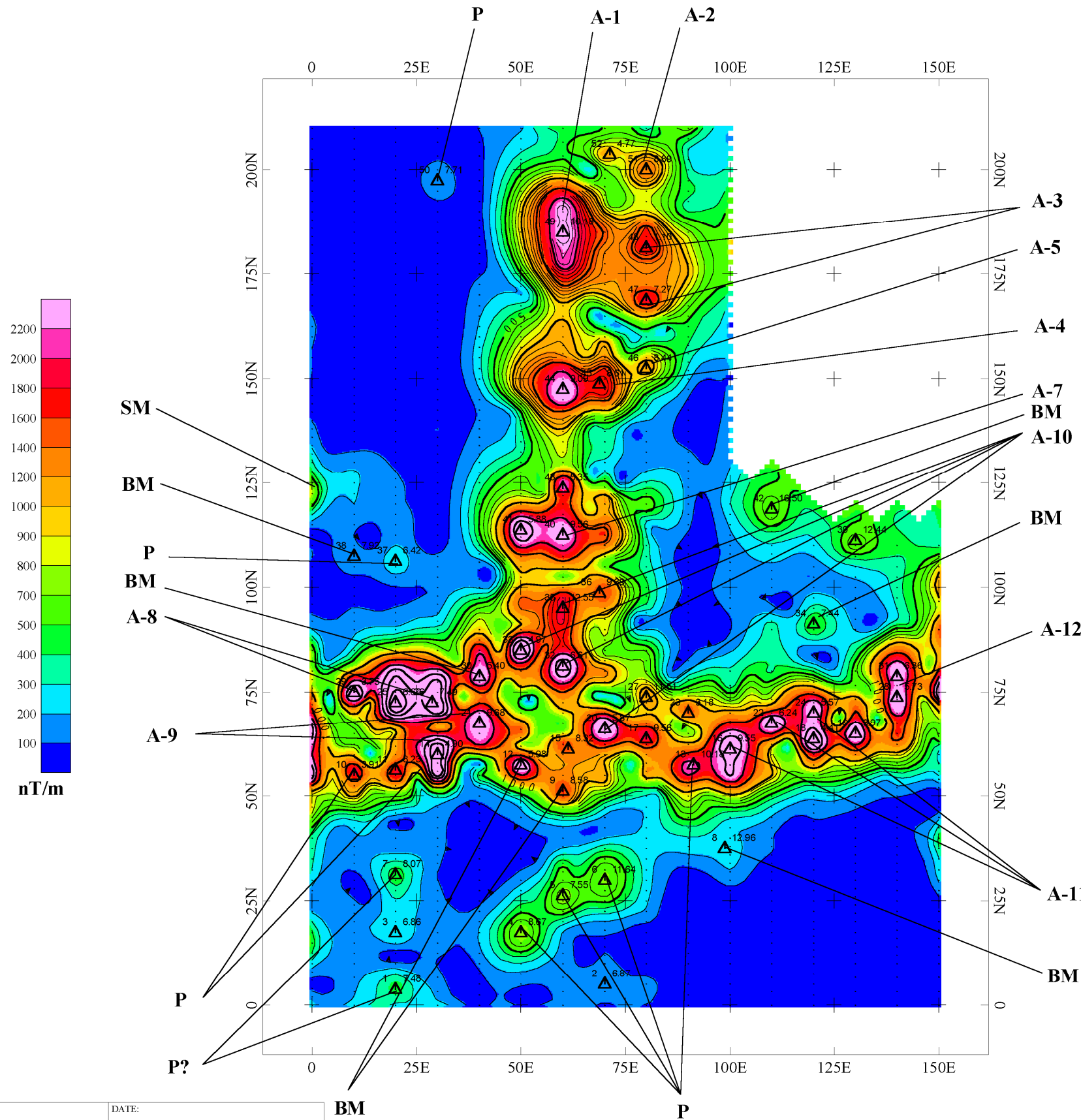
- A-1 GEOPHYSICAL ANOMALY DISCUSSED IN THE TEXT
- SM ANOMALY CAUSED BY SURFACE METAL
- BM ANOMALY CAUSED BY BURIED METAL
- RC ANOMALY CAUSED BY REINFORCED CONCRETE
- P ANOMALY CAUSED BY PIPE OR UTILITY
- F ANOMALY CAUSED BY FENCE
- B ANOMALY CAUSED BY BUILDING



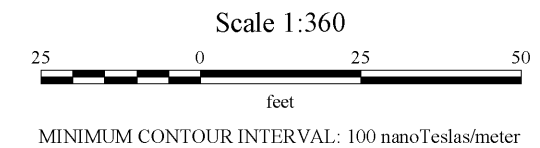
MINIMUM CONTOUR INTERVAL: 100 nanoTeslas

NAME: Sandra A. Takata	DATE: NOVEMBER 23, 1999.
PROJECT NUMBER: 774645	LOCATION: C:\FTMC\GSA\MGP\MAGU.map

**FIGURE A-3**  
**FORT McCLELLAN**  
**SITE - GSA WAREHOUSE**  
 G-858G TOTAL MAGNETIC FIELD  
 UPPER SENSOR (4.5 FT ABOVE GROUND SURFACE)  
 NORTH-SOUTH SURVEY LINES  
*IT GEOPHYSICS GROUP    KNOXVILLE, TENNESSEE*



- LEGEND:**
- A-1 GEOPHYSICAL ANOMALY DISCUSSED IN THE TEXT
  - SM ANOMALY CAUSED BY SURFACE METAL
  - BM ANOMALY CAUSED BY BURIED METAL
  - RC ANOMALY CAUSED BY REINFORCED CONCRETE
  - P ANOMALY CAUSED BY PIPE OR UTILITY
  - F ANOMALY CAUSED BY FENCE
  - B ANOMALY CAUSED BY BUILDING
  - △ Target ID    △ Target depth (ft)

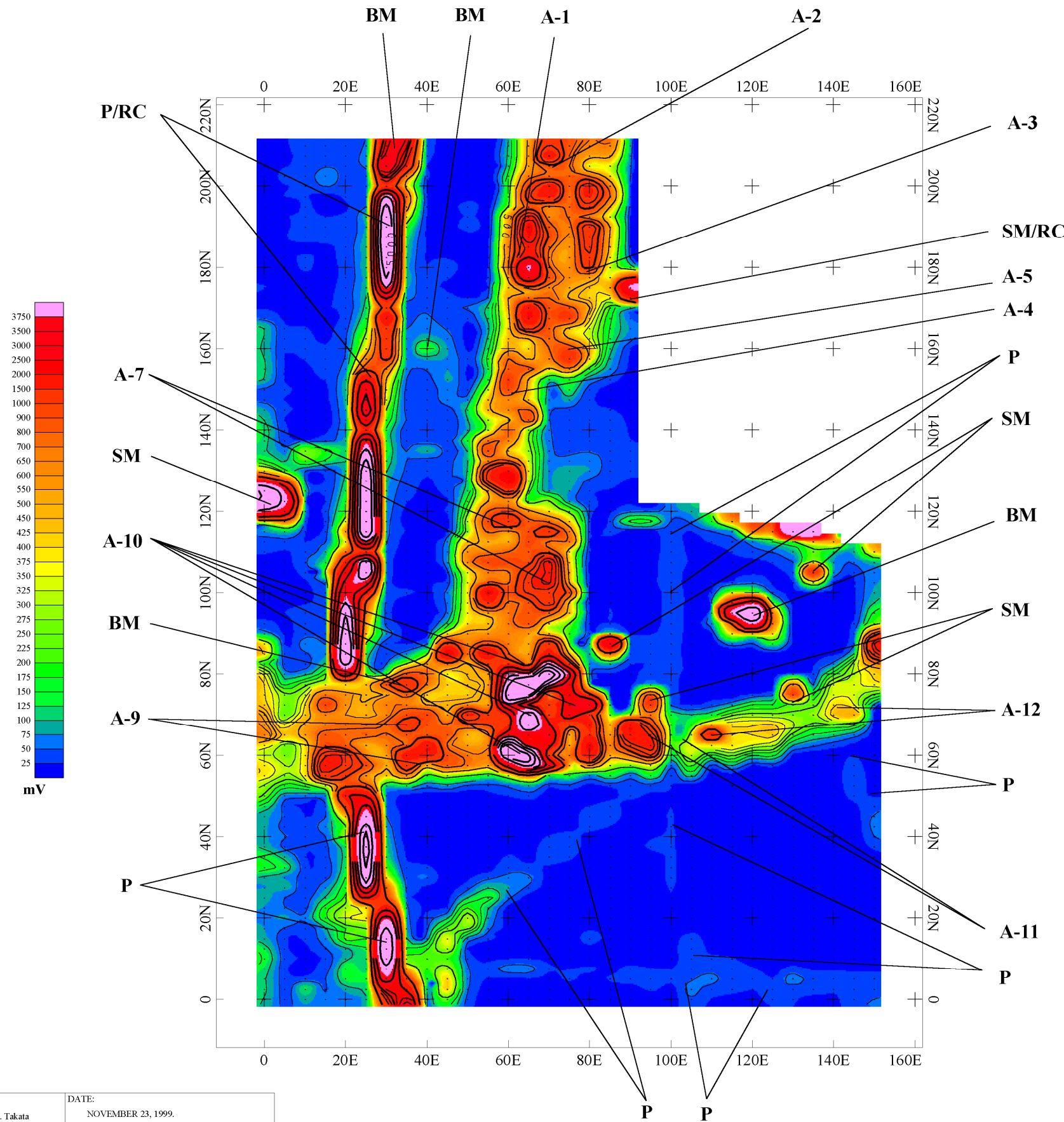


NAME: Sandra A. Takata	DATE: NOVEMBER 23, 1999.
PROJECT NUMBER: 774645	LOCATION: C:\FTMC\GSA\MGP\GSAAS

**FIGURE A-4**  
**FORT McCLELLAN**  
**SITE - GSA WAREHOUSE**

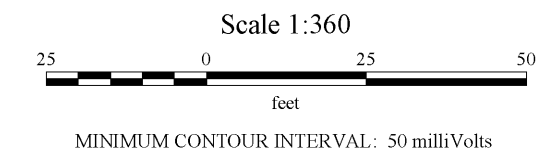
ANALYTIC SIGNAL  
G-858G UPPER SENSOR (4.5 FT ABOVE GROUND SURFACE)  
NORTH-SOUTH SURVEY LINES

**IT GEOPHYSICS GROUP    KNOXVILLE, TENNESSEE**



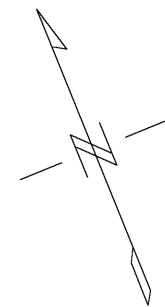
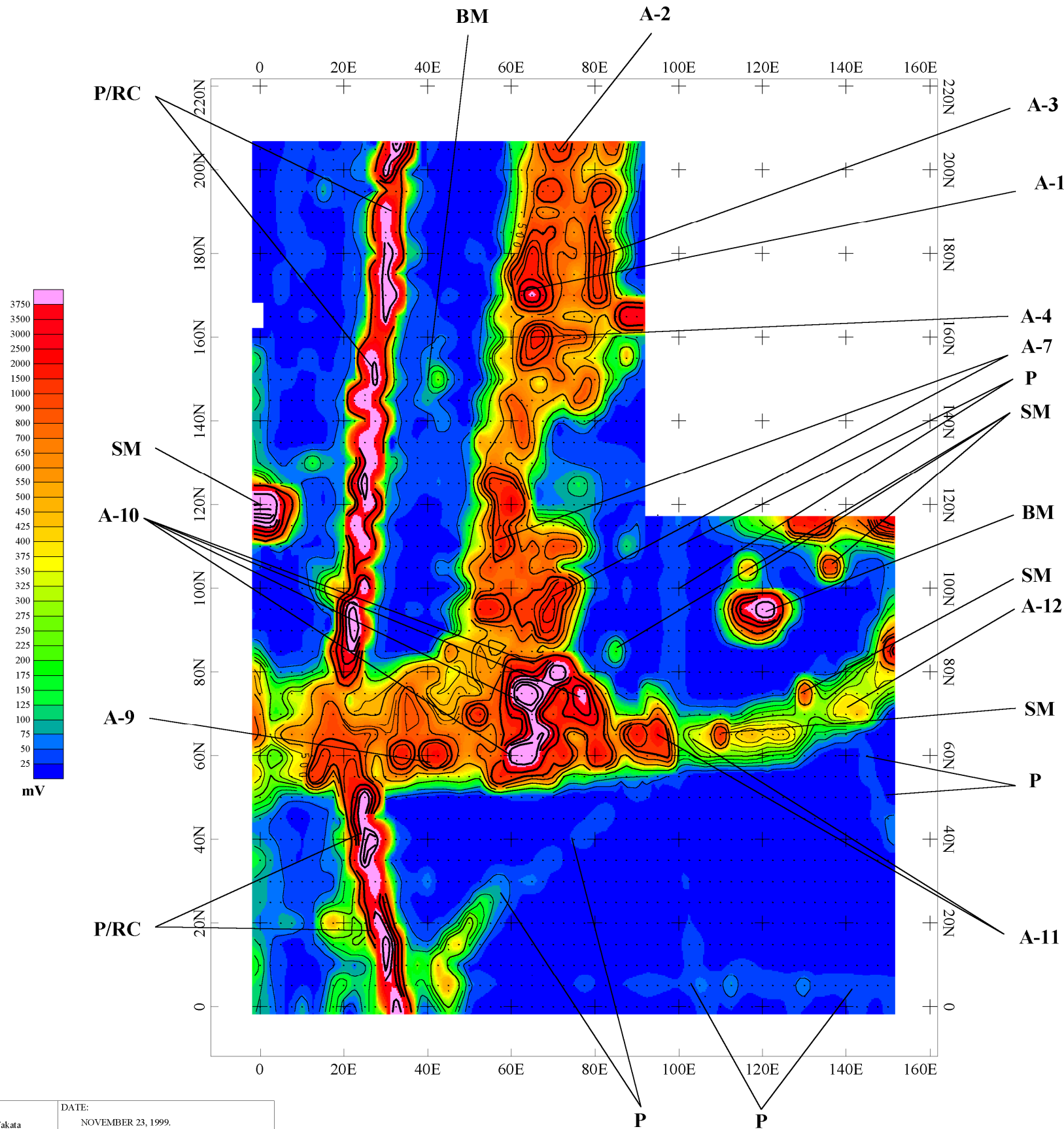
**LEGEND:**

- A-1 GEOPHYSICAL ANOMALY DISCUSSED IN THE TEXT
- SM ANOMALY CAUSED BY SURFACE METAL
- BM ANOMALY CAUSED BY BURIED METAL
- RC ANOMALY CAUSED BY REINFORCED CONCRETE
- P ANOMALY CAUSED BY PIPE OR UTILITY
- F ANOMALY CAUSED BY FENCE
- B ANOMALY CAUSED BY BUILDING



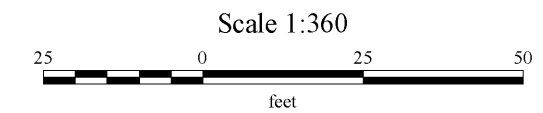
NAME: Sandra A. Takata	DATE: NOVEMBER 23, 1999.
PROJECT NUMBER: 774645	LOCATION: C:\FTMC\GSA\EM61\GSANB

**FIGURE A-5**  
**FORT McCLELLAN**  
**SITE - GSA WAREHOUSE**  
 EM61 POTENTIAL DIFFERENCE  
 BOTTOM COIL (1.5 FT ABOVE GROUND SURFACE)  
 NORTH-SOUTH SURVEY LINES  
*IT GEOPHYSICS GROUP KNOXVILLE, TENNESSEE*



**LEGEND:**

- A-1 GEOPHYSICAL ANOMALY DISCUSSED IN THE TEXT
- SM ANOMALY CAUSED BY SURFACE METAL
- BM ANOMALY CAUSED BY BURIED METAL
- RC ANOMALY CAUSED BY REINFORCED CONCRETE
- P ANOMALY CAUSED BY PIPE OR UTILITY
- F ANOMALY CAUSED BY FENCE
- B ANOMALY CAUSED BY BUILDING



MINIMUM CONTOUR INTERVAL: 50 milliVolts

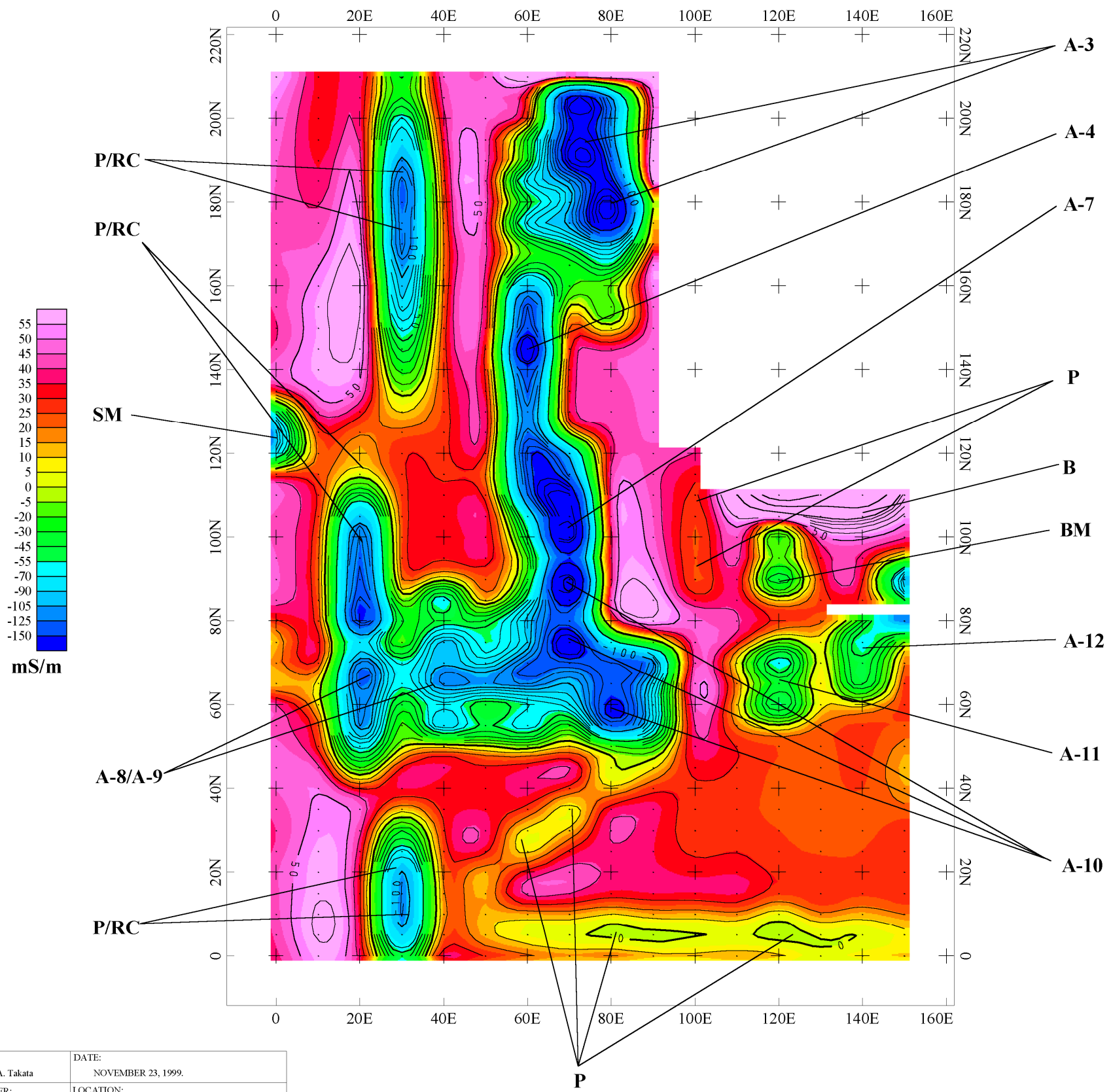
**FIGURE A-6**

**FORT McCLELLAN  
SITE - GSA WAREHOUSE**

EM61 POTENTIAL DIFFERENCE  
BOTTOM COIL (1.5 FT ABOVE GROUND SURFACE)  
EAST-WEST SURVEY LINES

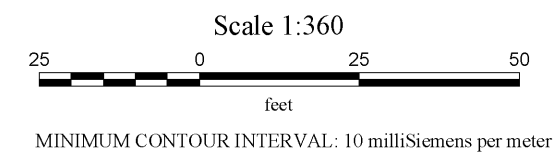
**IT GEOPHYSICS GROUP KNOXVILLE, TENNESSEE**

NAME: Sandra A. Takata	DATE: NOVEMBER 23, 1999.
PROJECT NUMBER: 774645	LOCATION: C:\FTMC\GSA\EM61\GSAEB



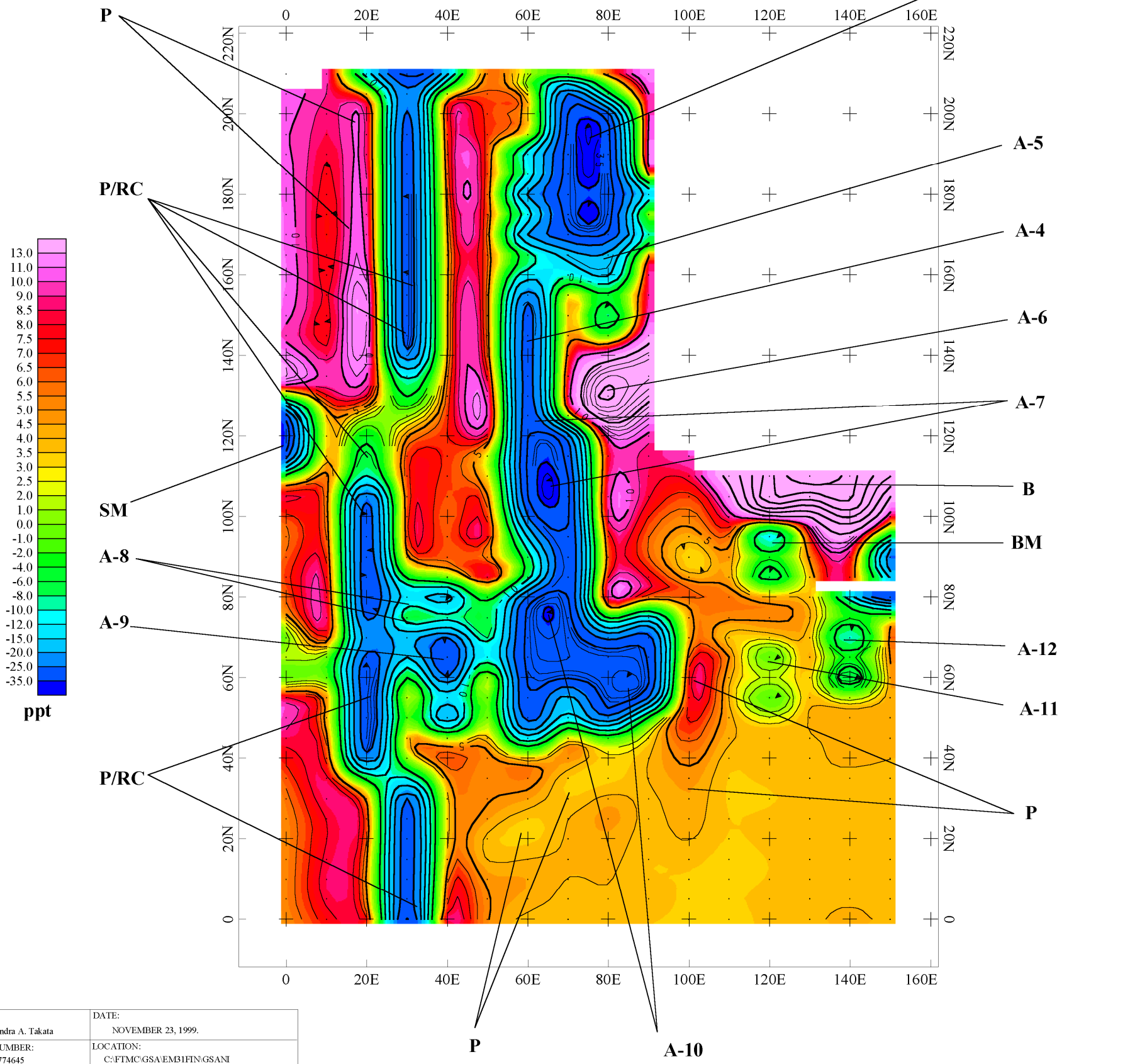
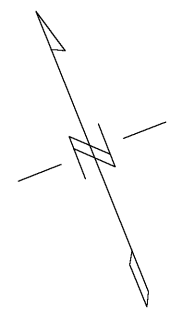
**LEGEND:**

- A-1 GEOPHYSICAL ANOMALY DISCUSSED IN THE TEXT
- SM ANOMALY CAUSED BY SURFACE METAL
- BM ANOMALY CAUSED BY BURIED METAL
- RC ANOMALY CAUSED BY REINFORCED CONCRETE
- P ANOMALY CAUSED BY PIPE OR UTILITY
- F ANOMALY CAUSED BY FENCE
- B ANOMALY CAUSED BY BUILDING



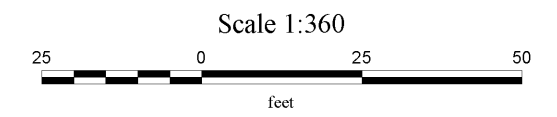
NAME: Sandra A. Takata	DATE: NOVEMBER 23, 1999.
PROJECT NUMBER: 774645	LOCATION: C:\FTMC\GSA\EMB1\FN\GSANC

**FIGURE A-7**  
**FORT McCLELLAN**  
**SITE - GSA WAREHOUSE**  
 EM31 CONDUCTIVITY  
 VERTICAL DIPOLE  
 NORTH-SOUTH SURVEY LINES  
*IT GEOPHYSICS GROUP KNOXVILLE, TENNESSEE*



**LEGEND:**

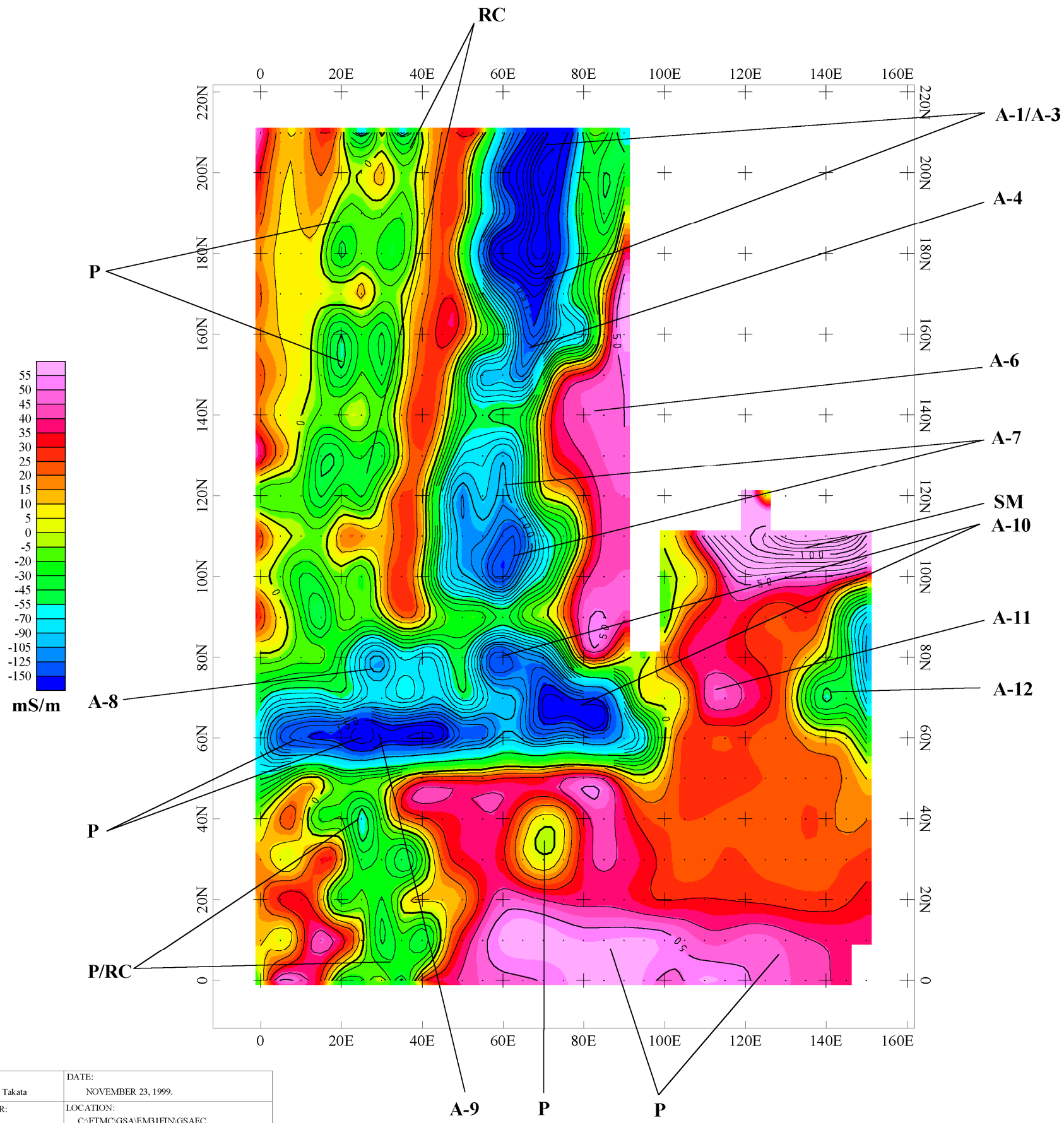
- A-1 GEOPHYSICAL ANOMALY DISCUSSED IN THE TEXT
- SM ANOMALY CAUSED BY SURFACE METAL
- BM ANOMALY CAUSED BY BURIED METAL
- RC ANOMALY CAUSED BY REINFORCED CONCRETE
- P ANOMALY CAUSED BY PIPE OR UTILITY
- F ANOMALY CAUSED BY FENCE
- B ANOMALY CAUSED BY BUILDING



MINIMUM CONTOUR INTERVAL: 1 ppt Secondary to Primary Field

NAME: Sandra A. Takata	DATE: NOVEMBER 23, 1999.
PROJECT NUMBER: 774645	LOCATION: C:\FTMC\GSA\EMB1\FIN\GSANI

**FIGURE A-8**  
**FORT McCLELLAN**  
**SITE - GSA WAREHOUSE**  
 IN-PHASE COMPONENT  
 EM31, VERTICAL DIPOLE  
 NORTH - SOUTH SURVEY LINES  
*IT GEOPHYSICS GROUP KNOXVILLE, TENNESSEE*



**LEGEND:**

- A-1 GEOPHYSICAL ANOMALY DISCUSSED IN THE TEXT
- SM ANOMALY CAUSED BY SURFACE METAL
- BM ANOMALY CAUSED BY BURIED METAL
- RC ANOMALY CAUSED BY REINFORCED CONCRETE
- P ANOMALY CAUSED BY PIPE OR UTILITY
- F ANOMALY CAUSED BY FENCE
- B ANOMALY CAUSED BY BUILDING



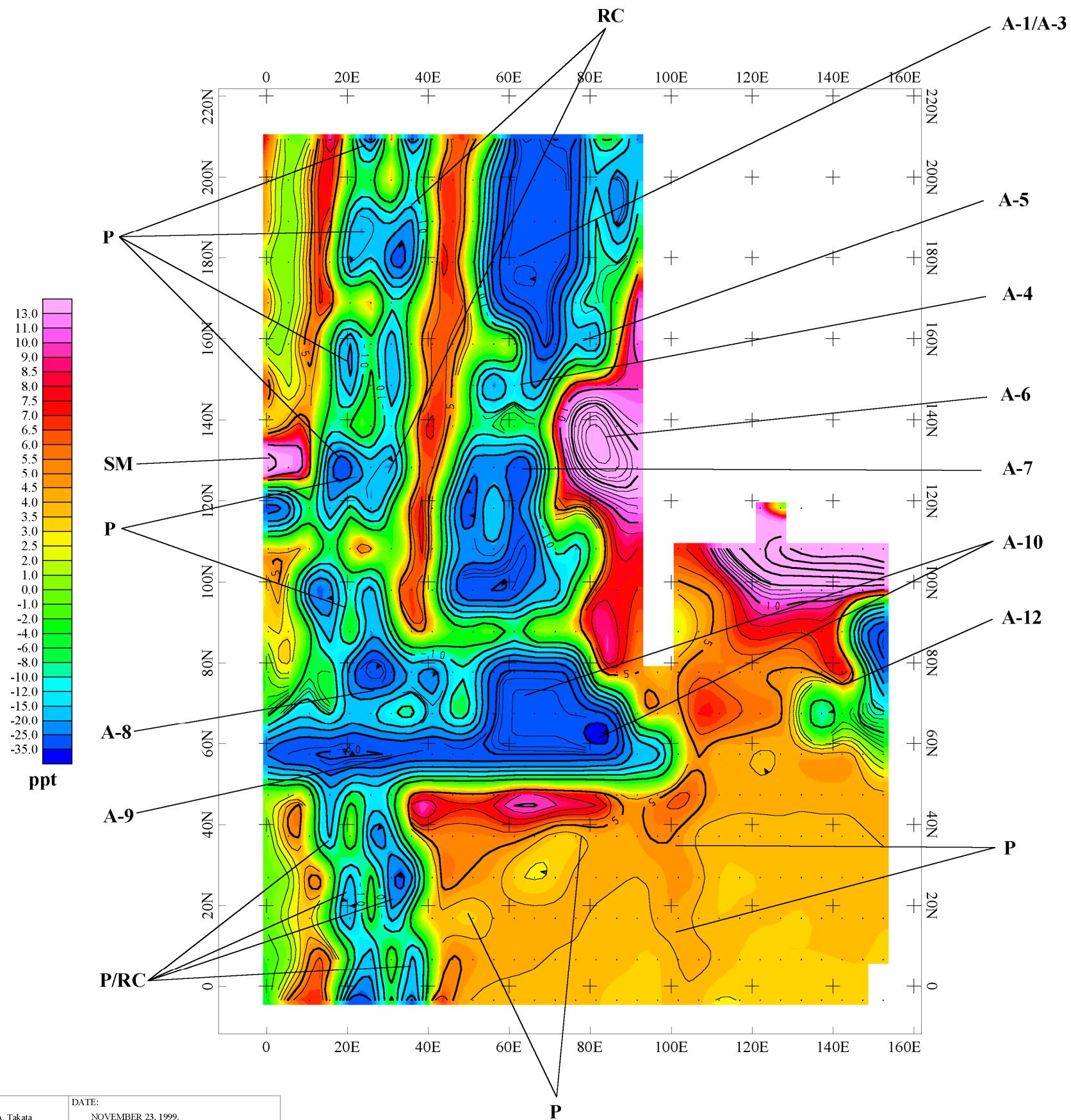
MINIMUM CONTOUR INTERVAL: 10 milliSiemens per meter

**FIGURE A-9**  
**FORT McCLELLAN**  
**SITE - GSA WAREHOUSE**

EM31 CONDUCTIVITY  
 VERTICAL DIPOLE  
 EAST-WEST SURVEY LINES

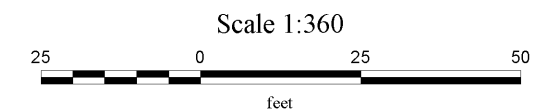
**IT GEOPHYSICS GROUP KNOXVILLE, TENNESSEE**

NAME: Sandra A. Takata	DATE: NOVEMBER 23, 1999.
PROJECT NUMBER: 774645	LOCATION: C:\FTMC\GSA\EMB1FIN\GSAEC



**LEGEND:**

- A-1 GEOPHYSICAL ANOMALY DISCUSSED IN THE TEXT
- SM ANOMALY CAUSED BY SURFACE METAL
- BM ANOMALY CAUSED BY BURIED METAL
- RC ANOMALY CAUSED BY REINFORCED CONCRETE
- P ANOMALY CAUSED BY PIPE OR UTILITY
- F ANOMALY CAUSED BY FENCE
- B ANOMALY CAUSED BY BUILDING



MINIMUM CONTOUR INTERVAL: 1 ppt Secondary to Primary Field

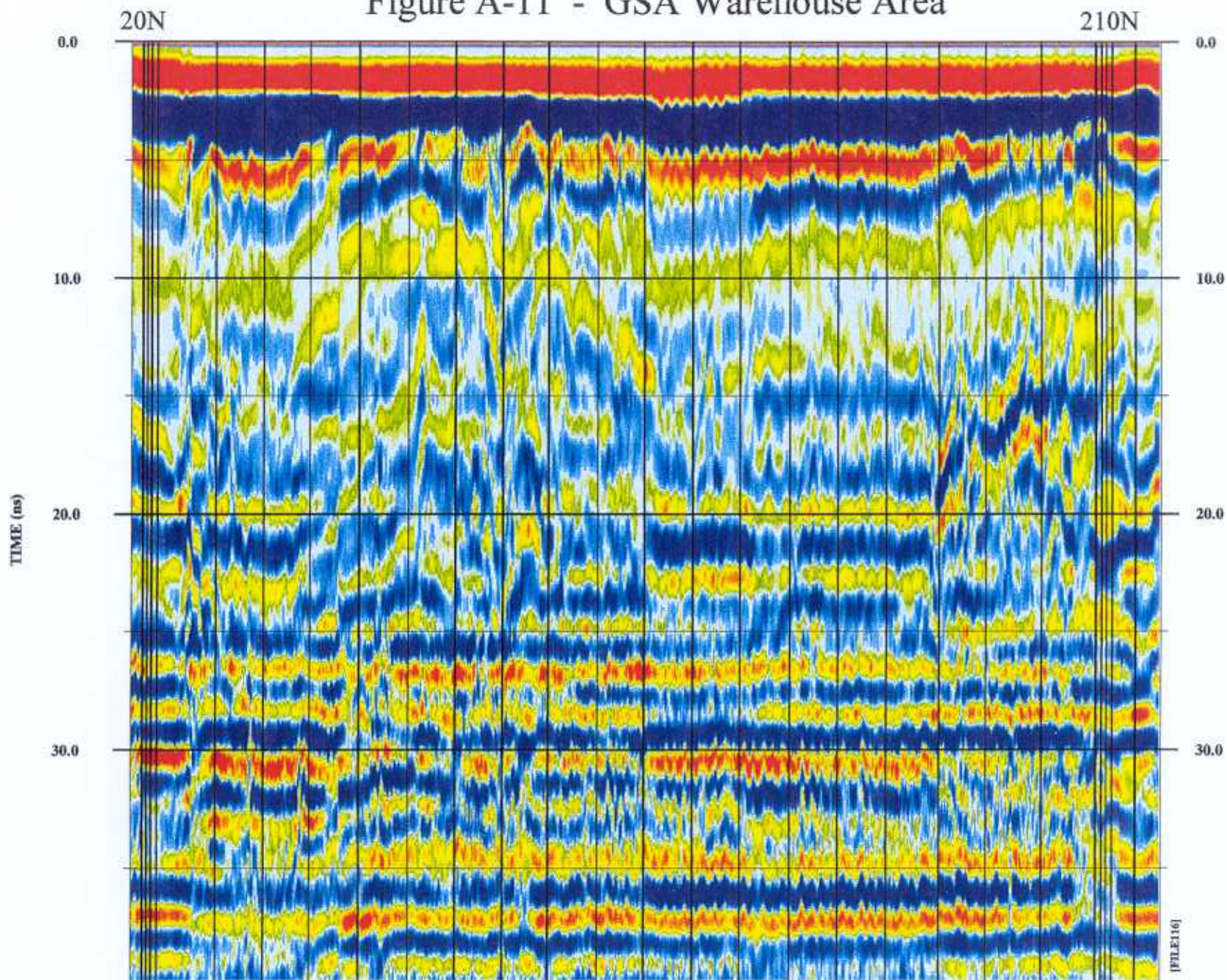
**FIGURE A-10**  
**FORT McCLELLAN**  
**SITE - GSA WAREHOUSE**

EM31 IN-PHASE COMPONENT  
 VERTICAL DIPOLE  
 EAST-WEST SURVEY LINES

**IT GEOPHYSICS GROUP KNOXVILLE, TENNESSEE**

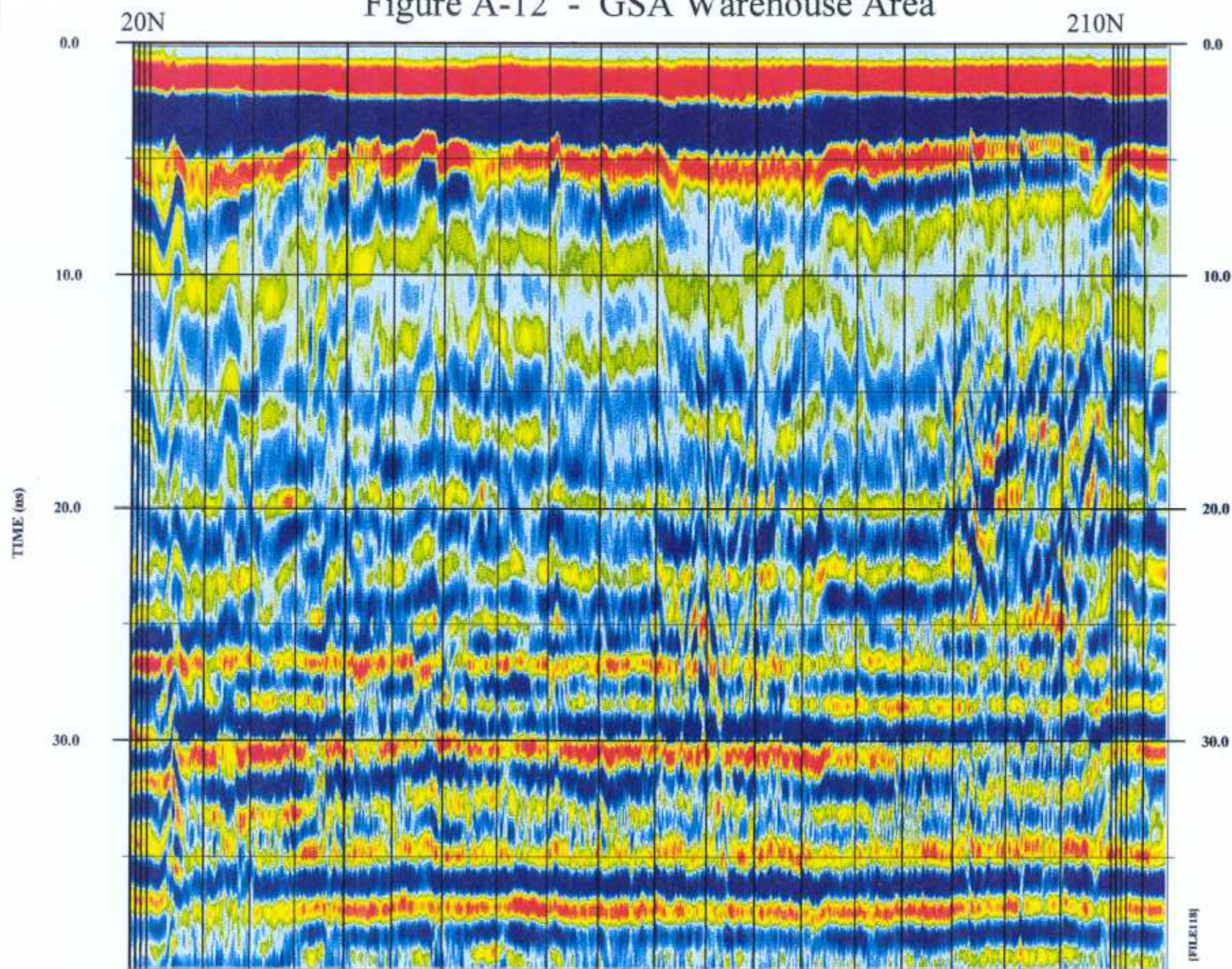
NAME: Sandra A. Takata	DATE: NOVEMBER 23, 1999.
PROJECT NUMBER: 774645	LOCATION: C:\FTMC\GSA\EMB1\FTN\GSAEI

Figure A-11 - GSA Warehouse Area



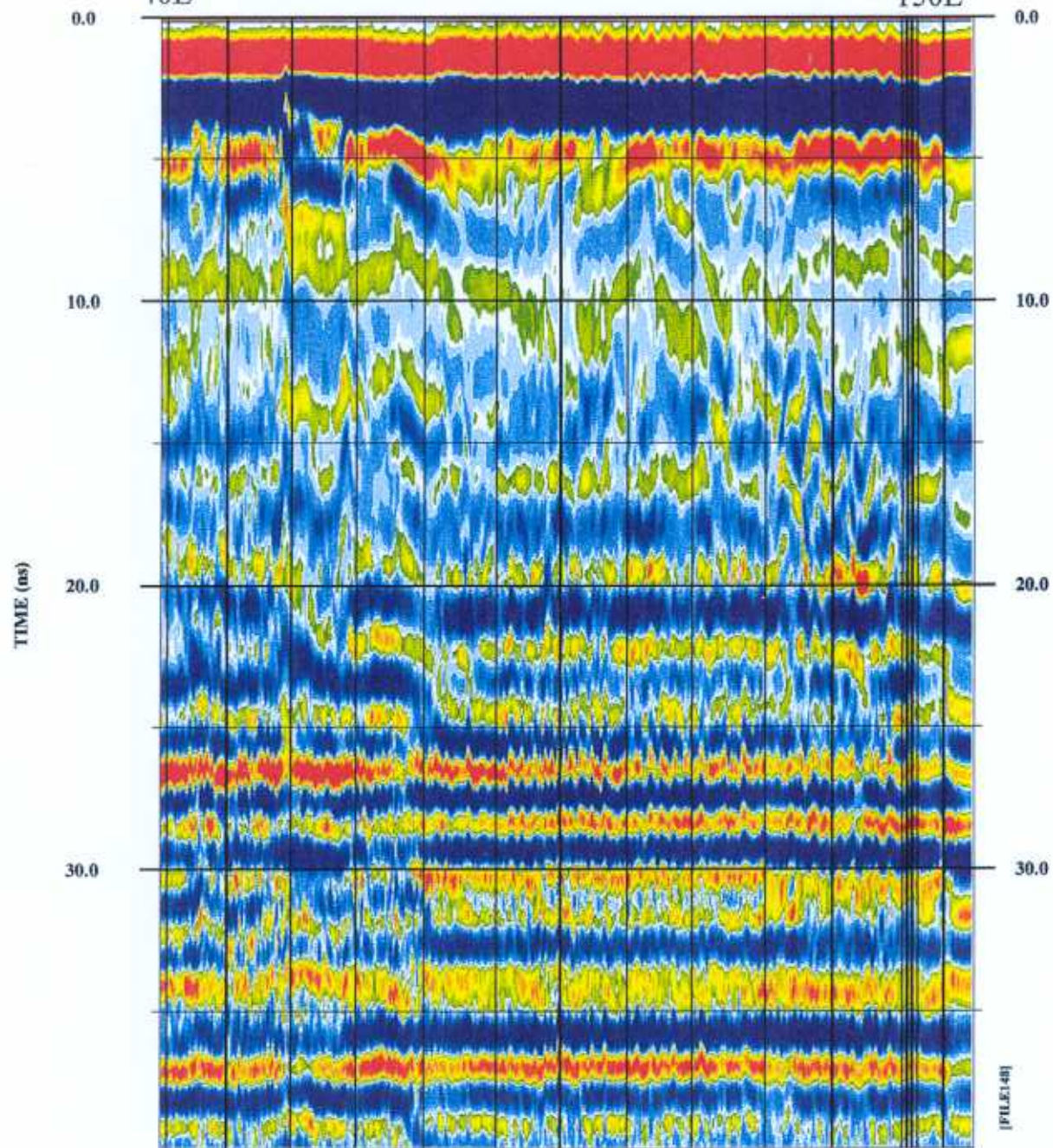
Line 65E, 400 MHz Antenna

Figure A-12 - GSA Warehouse Area



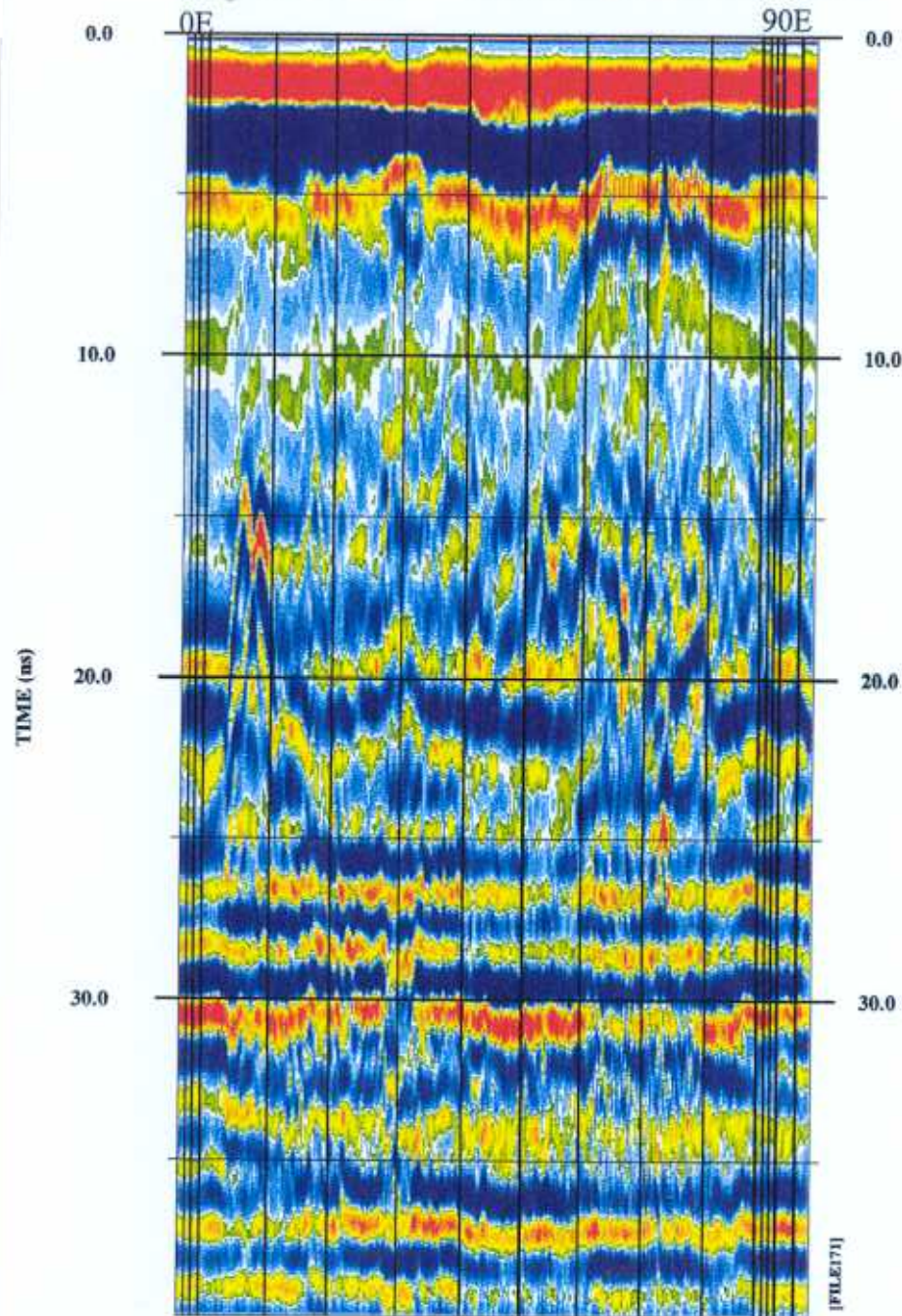
Line 75E, 400 MHz Antenna

40E Figure A-13 - GSA Warehouse Area 150E



Line 75N, 400 MHz Antenna

Figure A-14 - GSA Warehouse Area



Line180N, 400 MHz Antenna